PFC/JA-87-42

Microwave Plasma Diagnostics

H. Meuth
University of California
Berkeley, California 94720
and
E. Sevillano
Plasma Fusion Center
Massachusetts Institute of Technology
Cambridge, Massachusetts 02139

Supported by United States Department of Energy Contract DE-AC02-78ET51013.

TABLE OF CONTENTS

I. INTRODUCTION

Similar to optical diagnostics microwave plasma diagnostic techniques employ the measurement of (a) the wave reflection from, or, (b) the wave transmission through, or, (c) the wave absorption in a plasma, or any combination thereof (see Fig. 1). Exceptions to this are the case of interferometry, where only the effect of the plasma electron density upon the *phase* of the wave is of importance, and also the case of radiometry, whereby the plasma luminosity is recorded, and possibly spectrally resolved. But, unlike in optics, for reflection, transmission or absorption measurements in the microwave regime, the plasma is typically placed, or generated, in a cavity or a waveguide. Consequently, the goal of the measurement is to extract from the resulting loading effect some information about certain plasma properties, notably the *plasma density* and *collisionality*, and any properties associated with them.

At lower frequencies, up to about 1 GHz, commonly referred to as *rf frequencies*, the loading characteristics of a circuit element are mainly determined with the aid of a bridge circuit. This procedure presupposes that the element under investigation can be idealized as a single lumped circuit element. Resistors, capacitors, and inductors are common examples, that are measured with an LRC bridge. However, for the frequency range of *microwaves*, customarily defined as 1 GHz to 30 GHz (in the more restrictive sense of the word), free-space wavelengths are on the order of centimeters. The lumped circuit model has to be replaced more and more by a distributed circuit model, consisting of an array or network of individual components. Naturally, this applies even more so for *millimeter waves* for frequencies above 30 GHz. * The measurement circuits are basically of a bridge-type configuration, and, for many applications, are referred to as network analyzers (Masi and Phillips, 1986). There is a great number of such microwave bridge schemes, although they are variants of only a few basic designs. Hardware cost and technical support requirements can vary tremendously between a stand-alone cavity setup, or a one-channel interferometer for a small table-top plasma device, and, a fully computer-interfaced high-

* For the purpose here, we will always use the more loosely defined term *microwaves* for the entire frequency range of diagnostic interest.

power scattering apparatus or the multi-channel interferometer employed on present-day large scale machines for fusion research.

While waveguide and resonant-cavity experiments are typically performed at a few gigahertz, the range for interferometry extends to above 100 GHz; and microwave scattering and radiometry frequencies up to about 200 GHz are used in today's large fusion machines. Which frequency range to use depends to some extent on the parameters of the plasmas under investigation, especially for the latter two techniques.

Even after more than fourty years since the introduction of microwave techniques, their technology and engineering are still rapidly developing, nowadays particularly in the sector of active solid state devices (Morgan and Howes, 1980). Nevertheless, most of the components, like antennae, mixers, oscillators, amplifiers, detectors, and so on, are still serving essentially the same principal functions, just that some new diagnostic designs may have become more feasible. This fact will permit to emphasize the various diagnostic schemes that are commonly used, rather than their technological specifics. Moreover, there is ample, and also introductory literature available that has kept pace with new technological developments in the field (Gandhi, 1981; Bhartia and Bahl, 1984; Roddy, 1986). Analog and digital techniques for data acquisition, evaluation, and display have rapidly emerged and are now widely used, and some details will prove useful to the diagnostician.

In this chapter we restrict ourselves to the most commonly used microwave diagnostic techniques. The various sections are written such that they can be used independently. Prior to discussing the more experimental aspects of the various diagnostic methods in Sections III through V, a brief and basic, yet comprehensive introduction is given to waves in cold plasmas, with or without a static (i.e., time-constant) embedded magnetic field, as they apply to microwave diagnostics in a plasma. As in any diagnostic technique, the applied power levels are assumed to be small enough, so as not to alter the plasma properties. However, similar techniques can be used for *plasma formation and heating* at higher microwave power (Herlin and Brown, 1948; Asmussen *et al.*, 1974; Mejia *et al.*, 1985; Paraaszczak *et al.*, 1985). The latter is not part of the present chapter.

Finally, quite a number of books and survey articles exists, that cover some aspects of the subject presented here (Wharton, 1957, and 1965; Hermansdorfer, 1968; Podgornyi, 1971; Lisitano, 1975; Heald and Wharton, 1978; Golant, 1984; Luhmann and Peebles, 1984). This chapter should be considered as a complement that, however, will assume no background on plasma physics and that is intended for a larger audience of scientists and engineers performing research with any type of plasma. While in the past decades, plasma research was mainly directed towards the achievement of controlled fusion, many new and diverse applications have emerged very recently in material processing, or for the fabrication of integrated circuits (Chapman, 1980).

II. PLASMA WAVES AND THEIR APPLICATIONS IN MICROWAVE DIAGNOSTICS

Most treatises dealing with plasma waves usually discuss a variety of specific cases of waves. This is a consequence of the many parameters involved, that we enumerate here for electron plasma waves: the plasma angular frequency ω_p, that depends on the electron density n_e; the cyclotron frequency ω_c, depending on the magnetic field; and the collision frequency, ν_c, for electrons with other plasma particles or neutrals. Then, there is a set of wave numbers, or inversely, wavelengths, one parallel and generally two perpendicular to the static magnetic field vector, and the microwave frequency, $f = \omega/2\pi$. The electromagnetic wave fields are vectors characterized by their projections in and normal to the direction of propagation, or of the static magnetic field. All these mentioned quantities are interrelated according to propagation laws, or dispersion relations, and this allows that the plasma parameters, n_e and ν_c, can be inferred by measuring the propagation characteristics. If the plasma is spatially bounded, boundary conditions may significantly modify the wave dispersion. Such bounded plasmas are usually confined by metallic waveguides or cavities, commonly used for microwaves. A typical waveguide situation imposes the frequency, e.g. by an oscillator, and lets the wave numbers assume their permitted values. In a cavity, the wavelengths are set by the cavity dimensions, which therefore determine the resonant frequencies.

In this section, the propagation properties, i.e. the critical and resonance conditions,

are developed, as they are suitable for most diagnostic applications, invoking the cold plasma approximation, with or without an embedded homogeneous magnetic field. Both bounded and unbounded, homogeneous plasmas are considered, but as an exception, the inhomogeneous plasma column is also treated in Sect. II.E.4. The justifications for a homogeneous approximation are: (a) microwave measurements yield only a spatially integrated density or collision frequency; (b) with the above simplifications, the entire family of wave modes can be determined analytically.

While the earlier literature frequently gave results also in graphical form, this was omitted here. With today's widespread computerization, manipulation routines for, e.g. a 6×6 matrix, and Bessel functions of all kinds are readily available on libraries for computers of any performance level.

A. The Dielectric Tensor of a Cold Plasma

The dielectric tensor is a measure of response of a dielectric medium to external electric fields. To derive an explicit form for the dielectric tensor, we consider the case, where the plasma response is solely due to the plasma electrons, which move with the same speed. The first idealization implies that we are primarily interested in oscillatory electric fields of such high frequencies that the plasma ions with their much larger mass cannot follow these field oscillations. Microwaves are in this frequency range. The latter assumption precludes that the electrons have a sizable thermal motion of their own. Hence, the description addresses the cold plasma. While quite simplistic, these idealizations capture, to a large extent, the characteristics of the plasma response to external microwave fields.

We consider an electron of charge $-e$, and mass m, that moves under the influence of the Lorentz force in an electric field $\vec{\mathbf{E}}$ and a magnetic field $\vec{\mathbf{B}}$, with velocity $\vec{\mathbf{v}}$, and of a damping force proportional to $\vec{\mathbf{v}}$:

$$\frac{d\vec{\mathbf{v}}}{dt} = -\frac{e}{m}(\vec{\mathbf{E}} + \vec{\mathbf{v}} \times \vec{\mathbf{B}}) - \nu\vec{\mathbf{v}} \tag{1}$$

The damping is usually caused by collisions. The quantity ν can be identified in the simple picture presented here as a collision frequency, assumed to be velocity independent. We

are specifically interested in electromagnetic wave fields, i.e., we write $\vec{\mathbf{E}}$ and $\vec{\mathbf{B}}$ in terms of their Fourier amplitudes:

$$\vec{\mathbf{E}}(t) = \vec{\mathbf{E}}e^{i\omega t} \quad \text{(a)}, \quad \vec{\mathbf{B}}(t) = \vec{\mathbf{B}}_o + \vec{\mathbf{B}}e^{i\omega t} \quad \text{(b)} \tag{2}$$

We also assume $\vec{\mathbf{v}}$, $\vec{\mathbf{E}}$, and $\vec{\mathbf{B}}$ to be small compared with $\vec{\mathbf{B}}_o$. Then the second order term $\vec{\mathbf{v}} \times \vec{\mathbf{B}}$ may be ignored * and we can set $\vec{\mathbf{v}} \propto e^{i\omega t}$, to reduce Eq. (1) to an algebraic equation. This $\vec{\mathbf{v}} \times \vec{\mathbf{B}}$ term, and a second neglected nonlinear term, that also emerges from Eqs. (1) and (2), give rise to the ponderomotive force. It is of importance for the understanding of microwave *scattering* in a plasma, which will be discussed in Sec. V (Chen, 1984). Any DC electric fields are not considered in Eq. (2), because the high mobility of the charges inside the plasma tends to short out such fields, except in the edge regions (or sheaths) not considered here.

The alternating electronic motion of Eq. (1) results in an alternating current density $\vec{\mathbf{j}}$:

$$\vec{\mathbf{j}} = -en_e\vec{\mathbf{v}} = \overleftrightarrow{\sigma}\vec{\mathbf{E}}, \tag{3}$$

where n_e is the number density (m^{-3}) of the electrons, and $\overleftrightarrow{\sigma}$ is the (AC) conductivity tensor. Its tensor character arises from the cross product $\vec{\mathbf{v}} \times \vec{\mathbf{B}}_o = v_y B_o \hat{\mathbf{e}}_x - v_x B_o \hat{\mathbf{e}}_y$, where the z-axis is chosen along the direction of the (homogeneous) magnetic field $\vec{\mathbf{B}}_o$. An appropriate superposition of v_x and v_y, or j_x and j_y for that matter, will make $\overleftrightarrow{\sigma}$ diagonal:

$$X_{\left\{\begin{smallmatrix} L \\ R \end{smallmatrix}\right\}} = \frac{1}{\sqrt{2}}(X_x \mp iX_y) \leftrightarrow X_{\left\{\begin{smallmatrix} x \\ y \end{smallmatrix}\right\}} = \left\{\begin{smallmatrix} 1 \\ i \end{smallmatrix}\right\}\frac{1}{\sqrt{2}}(X_L \pm X_R) \tag{4}$$

In analogy to optics (Born and Wolf, 1980), the indices L and R stand for left and right circular polarization. Varying notations can be found in the literature, including unit vectors, which are self-orthogonal. With the transformation (4), the diagonalized conductivity tensor is made up of the elements:

$$\sigma_{\left\{\begin{smallmatrix} L \\ R \end{smallmatrix}\right\}} = -i\frac{\epsilon_o\omega_p^2}{\omega - i\nu \pm \omega_c} \quad ; \quad \sigma_P = -i\frac{\epsilon_o\omega_p^2}{\omega - i\nu}, \tag{5}$$

* More succinctly, we will consider the self-consistent electric and magnetic fields in the plasma, as they result from the plasma response to just these fields.

introducing the plasma frequency, ω_p, and the Larmor frequency, ω_c:

$$\omega_p^2 = \frac{n_e e^2}{\epsilon_o m} \tag{6}$$

$$\omega_c = \frac{eB_o}{m}. \tag{7}$$

The (relative) effective dielectric tensor, as it follows from Maxwell's equations (c.f. Sec. II.B), can then be expressed in the three diagonal elements:

$$\epsilon_{\left\{\begin{smallmatrix} L \\ R \\ P \end{smallmatrix}\right\}} = 1 - \frac{i}{\epsilon_o \omega} \sigma_{\left\{\begin{smallmatrix} L \\ R \\ P \end{smallmatrix}\right\}}. \tag{8}$$

In cartesian components, the dielectric tensor takes the form:

$$\overleftrightarrow{\epsilon} = \begin{pmatrix} S & -iD & 0 \\ iD & S & 0 \\ 0 & 0 & P \end{pmatrix}, \tag{9}$$

where

$$S = 1 - \frac{\omega_p^2(\omega - i\nu)}{\omega[(\omega - i\nu)^2 - \omega_c^2]}; \quad D = \frac{\omega_p^2 \omega_c}{\omega[(\omega - i\nu) - \omega_c^2]}; \quad P = 1 - \frac{\omega_p^2}{\omega(\omega - i\nu)}. \tag{10}$$

Figure 2 shows qualitatively these quantities as a function of ω, for $\nu = 0$. The zeros of S and P and the singularities of S, D, and P signify, non-propagation and bulk resonances in the plasma, respectively. In particular, the (longitudinal) dielectric constant P vanishes, given a certain frequency ω, and neglecting the collisionality ν, for a critical density n_c, for which:

$$n_c = \frac{\epsilon_o \omega^2 m}{e^2} \tag{11}$$

In terms of S, D, and P, the diagonalized tensor elements ϵ_L, ϵ_R and ϵ_P can be written as:

$$\epsilon_{\left\{\begin{smallmatrix} L \\ R \end{smallmatrix}\right\}} = S \pm D \quad ; \quad \epsilon_P = P. \tag{12}$$

B. Maxwell's Equations

The two homogeneous Maxwell's equations do not contain explicitly any currents or charges:

$$\nabla \times \vec{\mathbf{E}} = -\frac{\partial \vec{\mathbf{B}}}{\partial t} \tag{13}$$

$$\nabla \cdot \vec{\mathbf{B}} = 0. \tag{14}$$

The remaining two equations, in terms of current and charge densities, $\vec{\mathbf{j}}$ and ρ, and the relative dielectric tensor $\overleftrightarrow{\epsilon}$ according to Eqs. (3) and (8), read:

$$\nabla \times \vec{\mathbf{B}} = \mu_o(\vec{\mathbf{j}} + \epsilon_o \frac{\partial \vec{\mathbf{E}}}{\partial t}) = \mu_o \epsilon_o \frac{\partial \overleftrightarrow{\epsilon} \vec{\mathbf{E}}}{\partial t} \tag{15}$$

$$\nabla \cdot \epsilon_o \vec{\mathbf{E}} = \rho \tag{16}$$

By vector identity, we conclude from Eq. (15) that:

$$\nabla \cdot \overleftrightarrow{\epsilon} \vec{\mathbf{E}} = 0, \tag{17}$$

which is also a direct consequence of the continuity equation for the current, $\nabla \cdot \vec{\mathbf{j}} + \frac{\partial \rho}{\partial t} = 0$, and of Eq. (16). With $\vec{\mathbf{B}} = \mu_o \vec{\mathbf{H}}$, Eqs. (13) to (16) can be cast into the form,

$$-\nabla \times (\nabla \times \vec{\mathbf{E}}) = \mu_o \epsilon_o \frac{\partial^2 \overleftrightarrow{\epsilon} \vec{\mathbf{E}}}{\partial t^2} \tag{18}$$

$$-\nabla \times (\nabla \times \vec{\mathbf{H}}) = -\epsilon_o \frac{\partial \nabla \times \overleftrightarrow{\epsilon} \vec{\mathbf{E}}}{\partial t} \tag{19}$$

For waves in infinite plasmas the usual procedure is to expand $\vec{\mathbf{E}}$ and $\vec{\mathbf{H}}$ in plane waves with wave vector $\vec{\mathbf{k}}$, i.e., $\vec{\mathbf{E}}$, $\vec{\mathbf{H}} \propto e^{i(\omega t - \vec{\mathbf{k}} \cdot \vec{\mathbf{r}})}$. The operator $\nabla \times (\nabla \times\ )$ can then be replaced by $-\vec{\mathbf{k}} \times (\vec{\mathbf{k}} \times\ )$. The ensuing equation of the form $\overleftrightarrow{M} \vec{\mathbf{E}} = 0$ has only non-trivial solutions for $\vec{\mathbf{E}}$ when $||M|| = 0$, where M depends on $|\vec{\mathbf{k}}|$, the angle $(\vec{\mathbf{k}}, \vec{\mathbf{B}}_o)$, and the various elements of the dielectric tensor (Chen, 1984). The assumption of a plasma of infinite spatial dimension, and therefore, of plane waves, is justified, whenever the characteristic wavelength is much smaller than the extent of the plasma under investigation. However, for diagnostic purposes we are interested not only in plane wave propagation, but also in waves in bounded plasmas, as they occur in waveguides and cavities. There, e.g., the boundary conditions at curved surfaces will not admit plane wave solutions, as we will see in the subsequent sections. Still, essentially all configurations of diagnostic interest permit a plane wave expansion *along* the magnetic field direction. We pursue therefore, a more general approach that is akin to the one used in standard waveguide theory (see e.g. Gandhi, 1981). Since the goal is to provide formulae to interpret microwave measurements in plasmas, the plasma parameters and notably the dielectric tensor, are assumed to be

homogeneous but by no means isotropic. As an exception to this we also will treat a particular case where ϵ depends on the radius alone in Sec. II.E.4.

C. Wave Equations and Wave Solutions

1. Waves in a Magnetized Homogeneous Plasma

All vector quantities are separated into generally two perpendicular components and a parallel (or z-) component. For cartesian geometry one sets:

$$\vec{\mathbf{X}}(x,y,z,t) = (\vec{\mathbf{X}}_\perp(x,y) + X_z(x,y)\hat{\mathbf{e}}_z)e^{i(\omega t - kz)}, \tag{20}$$

while for cylindrical geometry one uses, instead:

$$\vec{\mathbf{X}}(r,\varphi,z,t) = (\vec{\mathbf{X}}_\perp(r) + X_z(r)\hat{\mathbf{e}}_z)e^{i(\omega t + m\varphi - kz)}. \tag{21}$$

The Fourier amplitudes $\vec{\mathbf{X}}_\perp$ and X_z carry still a tag for ω, k, and if applicable, for m. * In the following, the arguments (x,y) or (r), and the Fourier modulation factors will be omitted unless they are needed for clarity.

The z-components of Eqs. (18) and (19), respectively, turn, with the aid of Eqs. (9), and (13) through (17), into

$$(\nabla_\perp^2 - k^2\frac{P}{S} + \omega^2\mu_o\epsilon_o P)E_z = (\nabla_\perp^2 + \kappa_E^2)E_z = -i\omega k\frac{D}{S}\mu_o H_z \tag{22}$$

and

$$(\nabla_\perp^2 - k^2 + \omega^2\mu_o\epsilon_o\frac{S^2 - D^2}{S})H_z = (\nabla_\perp^2 + \kappa_H^2)H_z = i\omega k\frac{DP}{S}\epsilon_o E_z \tag{23}$$

with the transverse gradient defined, in analogy to Eqs. (20) and (21), as $\nabla_\perp = \nabla + ik\hat{\mathbf{e}}_z$. Equations (22) and (23) are coupled for E_z and H_z. As a consequence, in a magnetized plasma, generally *no pure TM or TE modes* familiar from (empty) waveguides and cavities *can exist.* Only for (a) electrostatic modes, where $\omega \to 0$, (b) modes at cutoff, where $k \to 0$, or (c) modes in unmagnetized plasmas where $D \to 0$, this classification *may* possibly still

* For comparison with the literature attention has to be paid to whether the Fourier modulation factors in (20), (21), or their conjugate complex are used.

be valid. However, the mixture of TE and TM modes that is here due to the bulk properties can also arise from a coupling in the boundary condition (c.f. Sec. II.D).

The longitudinal Eqs. (22) and (23) do not depend on any of the transverse components of the fields , and may thus be solved independently. Therefore, before proceeding to the transverse equations, we first observe some general properties of Eqs. (22) and (23). As long as $\omega k D/S \neq 0$, we can combine them in the two forms:

$$(\nabla_\perp^2 + \kappa_H^2)(\nabla_\perp^2 + \kappa_E^2)\left\{ \begin{matrix} E_z \\ H_z \end{matrix} \right\} = k_o^2 k^2 \frac{D^2 P}{S^2} \left\{ \begin{matrix} E_z \\ H_z \end{matrix} \right\}. \tag{24}$$

The wave number $k_o = \omega/c$ characterizes the free-space propagation with the speed of light $c = 1/\sqrt{\mu_o \epsilon_o}$. Anticipating the solutions of Eq. (24) in terms of Bessel functions for cylindrical geometry, or plane waves for cartesian geometry, we make the substitution $\nabla_\perp^2 \rightarrow -\kappa^2$, where κ is the transverse propagation constant. The two characteristic values for κ^2 follow from the now biquadratic Eq. (24) as

$$\kappa^2_{\left\{ \begin{matrix} 1 \\ 2 \end{matrix} \right\}} = \frac{1}{2}(\kappa_E^2 + \kappa_H^2) \pm \sqrt{\frac{1}{4}(\kappa_E^2 - \kappa_H^2)^2 + (k_o k \frac{D}{S})^2 P}. \tag{25}$$

In all generality, there will be four characteristic solutions to Eq. (24), the linear superposition of which will still have to obey the boundary conditions. The indices $\{1, 2\}$ in Eq. (25) were chosen such that for $k\omega/c = k k_o \rightarrow 0$, we have $\kappa_1^2 \rightarrow \kappa_E^2$, $\kappa_2^2 \rightarrow \kappa_H^2$. We mentioned already in Sec. II.A that for a critical density n_c, or for $P = 0$, the wave can no longer propagate, or, in other words, is cut off. This is, in view of Eqs. (22) and (23), only rigorously correct in the unmagnetized plasma. Another critical case follows from Eqs. (24) and (25), when two of the modes are *transversely* cut off, for which $\kappa^2 \rightarrow 0$. The condition for this to happen is

$$|k| = |k_o| \sqrt{\epsilon_{\left\{ \begin{matrix} L \\ R \end{matrix} \right\}}}, \tag{26}$$

which still describes propagation of plane waves along the magnetic field, with a modified speed characterized by the dielectric constants ϵ_L or ϵ_R given by Eqs. (12). Again, such modes may still be disallowed by the boundary conditons. Aside from plane waves, where

$\kappa = 0$, Eqs. (25) and (26) lead also to waves with non-trivial transverse wavenumbers:

$$\kappa^2_{\left\{\begin{smallmatrix} L \\ R \end{smallmatrix}\right\}} = \mp k^2 \frac{\epsilon_L - \epsilon_R}{\epsilon_L + \epsilon_R}(1 + \frac{\epsilon_P}{\epsilon_{\left\{\begin{smallmatrix} L \\ R \end{smallmatrix}\right\}}}). \tag{27}$$

We now specifically consider cylindrical geometry. There, the general non-singular solutions to Eq. (24) read, aside from a common Fourier modulation factor:

$$E_z = \sum_j J_m(\kappa_j r)\mathcal{E}_j \tag{28}$$

and

$$H_z = \sum_j J_m(\kappa_j r)\mathcal{H}_j. \tag{29}$$

The coefficients $\mathcal{E}$ and $\mathcal{H}$ are, by virtue of Eqs. (22) and (23), still subject to the relation

$$\mathcal{E}_j = e(\kappa_j)\mathcal{H}_j \tag{30}$$

or

$$\mathcal{H}_j = h(\kappa_j)\mathcal{E}_j, \tag{31}$$

where

$$e(\kappa_j) = -i\frac{S}{\epsilon_o \omega k D P}(\kappa_H^2 - \kappa_j^2) \tag{32}$$

and

$$h(\kappa_j) = i\frac{S}{\mu_o \omega k D}(\kappa_E^2 - \kappa_j^2). \tag{33}$$

Clearly, from Eqs. (24) and (25), one gets $e(\kappa_j)h(\kappa_j) = 1$. In the limiting case $\omega k \to 0$, one has $h(\kappa_1) \to 0; |h(\kappa_2)| \to \infty; |e(\kappa_1)| \to \infty$, and $e(\kappa_2) \to 0$. Regarding the solutions (28) and (29), any basis of coefficients $(\mathcal{H}_1, \mathcal{H}_2)$, or $(\mathcal{E}_1, \mathcal{E}_2)$, or $(\mathcal{E}_1, \mathcal{H}_2)$, or $(\mathcal{E}_2, \mathcal{H}_1)$ may be chosen, while all others follow via Eqs. (30) to (33).

The equations for the transverse components can be cast into the following form, making use of Eqs. (13) through (17), and the symmetry properties of $\overleftrightarrow{\epsilon}$

$$(k_o^2 \overleftrightarrow{\epsilon}_\perp - k^2 \overleftrightarrow{I}_\perp)\vec{\mathbf{E}}_\perp = -ik\nabla_\perp E_z + i\mu_o\omega(\hat{\mathbf{e}}_z \times \nabla_\perp)H_z \tag{34}$$

and

$$(k_o^2 \overleftrightarrow{\epsilon}_\perp - k^2 \overleftrightarrow{I}_\perp)\vec{\mathbf{H}}_\perp = -ik\nabla_\perp H_z - i\epsilon_o\omega \overleftrightarrow{\epsilon}_\perp(\hat{\mathbf{e}}_z \times \nabla_\perp)E_z. \tag{35}$$

The subscript $\perp$ refers again to the (x, y) or (r, φ) components only, and $\overleftrightarrow{I}$ is the unit diagonal tensor. Therefore, once the solutions for E_z and H_z have been determined from Eqs. (22), (23), (24) and (28) through (33), the inhomogeneous particular solutions for all the transverse components can be constructed. In Eqs. (34) and (35), we encounter again the component mixing property of the cross product. It can be disentangled by a complex principal axis transformation of the sort of Eq. (4), that can also be written in cylindrical coordinates:

$$X_{\left\{\begin{smallmatrix} L \\ R \end{smallmatrix}\right\}} = \frac{1}{\sqrt{2}} e^{\mp i\varphi}(X_r \mp iX_\varphi) \leftrightarrow X_{\left\{\begin{smallmatrix} r \\ \varphi \end{smallmatrix}\right\}} = \left\{\begin{smallmatrix} 1 \\ i \end{smallmatrix}\right\} \frac{1}{\sqrt{2}}(X_L e^{i\varphi} \pm X_R e^{-i\varphi}). \tag{36}$$

In any case, independently of the geometry chosen, Eqs. (34) and (35) readily reduce, also by virtue of Eqs. (20) or (21), to the four algebraic equations for E_L, E_R, H_L and H_R:

$$\left\{\begin{smallmatrix} E_\ell \\ H_\ell \end{smallmatrix}\right\} = \frac{1}{k_o^2\epsilon_\ell - k^2}\partial_\ell\left(-ik\left\{\begin{smallmatrix} E_z \\ H_z \end{smallmatrix}\right\} \pm \omega s_\ell \left\{\begin{smallmatrix} \mu_o H_z \\ \epsilon_o\epsilon_\ell E_z \end{smallmatrix}\right\}\right) \tag{37}$$

where $\ell = \{L, R\}$, and $s_L = +1, s_R = -1$. The differential operator ∂_ℓ, acting on the known functions E_z and H_z, is defined in analogy to Eqs. (4) and (36). In particular, for cylindrical geometry, one has

$$\partial_\ell \mathcal{C}_m(\kappa r)e^{im\varphi} = \langle s_\ell \rangle \frac{\kappa}{\sqrt{2}} \mathcal{C}_{m-s_\ell}(\kappa r)e^{i(m-s_\ell)\varphi}. \tag{38}$$

The $\mathcal{C}_m$'s stand for any cylinder function $J_m, Y_m, I_m, e^{im\pi}K_m$ (for the latter two modified cylinder functions the factor $\langle s_\ell \rangle$ on the RHS is to be omitted). For cartesian geometry, the action of ∂_ℓ on plane waves is trivial via the substitution $\partial_\ell \to (-1/\sqrt{2})(ik_x + s_\ell k_y)$. In microwave plasma diagnostics, the most common configuration is cylindrical, to which in what follows, we will restrict ourselves. The cartesian or slab configuration can be dealt with analogously with the simpler property of ∂_ℓ, or by the plane wave method discussed in Sect. II.B.

On the basis of Eqs. (28), (29), (36), and (38), we find the solutions to Eq. (37) in terms of the radial and azimuthal components.

$$E_{\left\{\begin{smallmatrix} r \\ \varphi \end{smallmatrix}\right\}} = \sum_j (k\mathcal{A}_{\left\{\begin{smallmatrix} 1 \\ 2 \end{smallmatrix}\right\}}(\kappa_j, r) \pm \omega\mu_o \mathcal{A}_{\left\{\begin{smallmatrix} 2 \\ 1 \end{smallmatrix}\right\}}(\kappa_j, r) h(\kappa_j)) \mathcal{E}_j \tag{39}$$

and

$$H_{\left\{\begin{smallmatrix} r \\ \varphi \end{smallmatrix}\right\}} = \sum_j (k\mathcal{A}_{\left\{\begin{smallmatrix} 1 \\ 2 \end{smallmatrix}\right\}}(\kappa_j, r) + \omega\epsilon_o \mathcal{B}_{\left\{\begin{smallmatrix} 1 \\ 2 \end{smallmatrix}\right\}}(\kappa_j, r) e(\kappa_j)) \mathcal{H}_j, \tag{40}$$

that still have to be subjected to Eqs. (30) to (33). The radial dependency is in the functional coefficients $\mathcal{A}(\kappa_j, r), \mathcal{B}(\kappa_j, r)$:

$$\mathcal{A}_{\left\{\begin{smallmatrix} 1 \\ 2 \end{smallmatrix}\right\}}(\kappa, r) = -\frac{i\kappa}{2} \sum_{\ell=L,R} \left\{\begin{smallmatrix} s_\ell \\ i \end{smallmatrix}\right\} \frac{J_{m-s_\ell}(\kappa r)}{k_o^2 \epsilon_\ell - k^2} \tag{41}$$

$$\mathcal{B}_{\left\{\begin{smallmatrix} 1 \\ 2 \end{smallmatrix}\right\}}(\kappa, r) = -\frac{\kappa}{2} \sum_{\ell=L,R} \left\{\begin{smallmatrix} 1 \\ is_\ell \end{smallmatrix}\right\} \frac{\epsilon_\ell J_{m-s_\ell}(\kappa r)}{k_o^2 \epsilon_\ell - k^2}. \tag{42}$$

These sums can be expanded in terms of J_m and $J'_m = \frac{dJ_m(x)}{dx}$. For this we recall that $s_L = +1, s_R = -1$, and make use of standard recursion relations for cylinder functions, and of Eqs. (12), (22) and (23):

$$\left\{\begin{matrix} \mathcal{A}_1(\kappa, r) \\ \mathcal{A}_2(\kappa, r) \end{matrix}\right\} = -\frac{i\kappa \frac{S}{P}}{k_o^2(\kappa_H^2 - k^2)S + k^4} \begin{pmatrix} \kappa_E^2 & ik_o^2 \frac{PD}{S} \\ -ik_o^2 \frac{PD}{S} & \kappa_E^2 \end{pmatrix} \times \left\{\begin{matrix} J'_m(\kappa r) \\ \frac{im}{\kappa r} J_m(\kappa r) \end{matrix}\right\} \tag{43}$$

$$\left\{\begin{matrix} \mathcal{B}_1(\kappa, r) \\ \mathcal{B}_2(\kappa, r) \end{matrix}\right\} = \frac{\kappa S}{k_o^2(\kappa_H^2 - k^2)S + k^4} \begin{pmatrix} k^2 \frac{D}{S} & i\kappa_H^2 \\ -i\kappa_H^2 & k^2 \frac{D}{S} \end{pmatrix} \times \left\{\begin{matrix} J'_m(\kappa r) \\ \frac{im}{\kappa r} J_m(\kappa r) \end{matrix}\right\}. \tag{44}$$

The $\times$-product is to be understood between the matrix () and the column {}.

Equations (28) and (29), in conjunction with Eqs. (30) to (33), and Eqs. (39) and (40), in conjunction with Eqs. (41) to (44), constitute the entire family of solutions of waves in a cold plasma, suitable for cylindrical geometry. To construct a specific solution, their linear superposition has to obey the boundary conditions, which will be addressed in Sect. II.D.

2. Guided Electromagnetic Waves in Vacuum

Prior to that we shall briefly quote the wave solutions in a vacuum layer between

the plasma edge and the wall. They are of importance for the propagation and resonance properties in waveguides or cavities that are only partially filled with plasma. Along the very same lines as in the preceding section, however, with the simplification that now $D = 0, P = S = 1$, we can expand the solutions in the form

$$\begin{Bmatrix} E_z^v \\ H_z^v \end{Bmatrix} = \sum_i \begin{Bmatrix} \mathcal{F}_i \\ \mathcal{G}_i \end{Bmatrix} C_m^{(i)}(\kappa_v r), \tag{45}$$

where $C_m^{(1,2)} = (J_m, Y_m)$ are the regular and singular Bessel functions; and the vacuum transverse propagation constant is given by $\kappa_v^2 = \omega^2/c^2 - k^2 = k_o^2 - k^2$. The common Fourier modulation factors were omitted in Eq. (45). The resulting transverse components are then:

$$E^v_{\begin{Bmatrix} r \\ \varphi \end{Bmatrix}} = \sum_i (k\mathcal{K}^i_{\begin{Bmatrix} 1 \\ 2 \end{Bmatrix}} \mathcal{F}_i \pm \omega\mu_o \mathcal{K}^i_{\begin{Bmatrix} 2 \\ 1 \end{Bmatrix}} \mathcal{G}_i) \tag{46}$$

and

$$H^v_{\begin{Bmatrix} r \\ \varphi \end{Bmatrix}} = \sum_i (\mp\omega\epsilon_o \mathcal{K}^i_{\begin{Bmatrix} 2 \\ 1 \end{Bmatrix}} \mathcal{F}_i + k\mathcal{K}^i_{\begin{Bmatrix} 1 \\ 2 \end{Bmatrix}} \mathcal{G}_i) \tag{47}$$

with the radial functions $\mathcal{K}$ given in terms of the Bessel functions and their derivatives:

$$\mathcal{K}_1^i(\kappa_v r) = -\frac{i}{\kappa_v} C_m^{(i)\prime}(\kappa_v r) \quad \text{and} \quad \mathcal{K}_2^i(\kappa_v r) = \frac{m}{\kappa_v^2 r} C_m^{(i)}(\kappa_v r). \tag{48}$$

D. Boundary Conditions

The boundary conditions follow directly from integrating Maxwell's equations through any arbitrary interface, and are therefore consistent with the wave equations of Sect. II.C. However, since not only Maxwell's equations, but also the equation of motion for the electron plasma, Eq. (1), were used, caution has to be exercised. Any sufficient and linearly independent set of conditions that is consistent with both Maxwell's equations and the equation of motion may be chosen to uniquely determine the wave solutions.

1. General Conditions

We consider first the conditions resulting from Maxwell's equations (13) and (14): They require that, on any physical or fictitious surface, characterized by its local normal

vector $\hat{\mathbf{n}}$, the normal component of the magnetic field and the tangential component of the electric field be continuous:

$$\hat{\mathbf{n}} \cdot (\vec{\mathbf{B}}^{<} - \vec{\mathbf{B}}^{>}) = 0 \quad ; \quad \hat{\mathbf{n}} \times (\vec{\mathbf{E}}^{<} - \vec{\mathbf{E}}^{>}) = 0. \tag{49}$$

Equation (15) leads to

$$\hat{\mathbf{n}} \times (\vec{\mathbf{B}}^{<} - \vec{\mathbf{B}}^{>}) = -\mu_o \vec{\mathbf{I}}_s. \tag{50}$$

Unlike in hot plasmas, there is no singular surface current in a cold plasma, i.e., $\vec{\mathbf{I}}_s = 0$. Equation (17) yields the requirement for the quantity $\hat{\mathbf{n}} \cdot (\overleftrightarrow{\epsilon}\vec{\mathbf{E}})$ to be continuous. For a cylindrical boundary of radius r_o where $\hat{\mathbf{n}} = \hat{\mathbf{e}}_r$, this implies that

$$SE_r^{<} - iDE_\varphi^{<} = E_r^{>} \quad \text{at} \quad r = r_o, \tag{51}$$

which in the isotropic unmagnetized case, where $D \equiv 0, S = P$, reduces to the condition familiar from electrostatics: $PE_r^{<} = E_r^{>}$ at $r = r_o$. Equation (51) neglects the presence of any surface charge Σ, for if we consider Ohm's law through the surface, $j_r = [\overleftrightarrow{\sigma}\vec{\mathbf{E}}]_r$, the current has to drop instantly to zero at $r = r_o + \delta$. This will lead to charge build-up according to the continuity equation $\nabla \cdot \vec{\mathbf{j}} + \frac{\partial \rho}{\partial t} = 0$. Consequently, the electrostatic solution (51) may not be used to determine the solution.

We briefly point out the importance of the surface charge for the coupling of waves in the boundary: the resulting charge distribution in the surface is such that, whenever there exists a wave mode with finite axial wavelength (i.e., $k \neq 0$), *radial electric fields* will always be accompanied by *axial electric fields* (and vice versa), as they are induced by the plasma vacuum boundary. And it is so regardless of whether the static magnetic field is zero or not. This situation is schematically depicted in Fig. 3. A similar statement applies for any non-zero azimuthal mode number (i.e., $m \neq 0$). It should be recalled that the bulk properties of the plasma lead to such coupling only for a non-zero magnetic field (c.f. Sect. II.C.1). Even if the physically more reasonable assumption is made that the electrons may move across the boundary, the situation still remains the same, as can be argued from Fig. 3(b). In reality, there is never such a sharp plasma edge. But even in

a more diffuse plasma-vacuum transition, a polarization charge is induced and the above applies at least qualitatively. If the plasma however, is in contact with a conducting wall, then the axial E-fields are largely shorted out, as will be discussed now.

2. Conditions on a Conducting Wall

At an infinitely conducting wall, Eq. (49) reduces to

$$\hat{\mathbf{n}} \cdot \vec{\mathbf{B}}^{<} \to 0 \quad ; \quad \hat{\mathbf{n}} \times \vec{\mathbf{E}}^{<} \to 0, \tag{52}$$

since no electric field, nor any oscillatory magnetic field may exist inside the conductor. For waveguides or cavities, where the plasma is not in contact with the conducting wall, the boundary condition $\frac{\partial B_z}{\partial r}(r = r_c) = 0$ is also used (Jackson, 1975). More generally, from the φ-component of Eq. (15) we have, invoking the conditions (52), for a plasma in contact with the wall

$$\frac{\partial B_z}{\partial r} = \frac{1}{2}\omega\mu_o\epsilon_o(\epsilon_L - \epsilon_R)E_r = \frac{1}{2}\omega\mu_o\epsilon_o D E_r, \quad \text{at} \quad r = r_c. \tag{53}$$

The RHS vanishes for a non-magnetized plasma, just as in the case for the empty waveguide.

The discussion so far concerned explicitly the boundary conditions in transverse directions. The boundary conditions (49) and (52), applied in axial direction, where $\hat{\mathbf{n}}$ is parallel to the z-axis, are easily met by an appropriate superposition of the axial plane waves. Clearly, considering the symmetry properties of Eqs. (28), (29), (39), (40), (45), (46) and (47), with respect to the change of sign of k, solutions can always be constructed such that, say, $H_z, E_r, E_\varphi \propto \sin kz$ and $E_z, H_r, H_\varphi \propto \cos kz$ to ensure that the field projections (52) vanish. It is, therefore, not necessary to differentiate between running waves, as they occur in waveguides that are not subject to axial conditions, and standing waves, that occur in an axially bounded plasma in a cavity, with, however, one exception: for $k = 0$, the situation is different. As a result, TE_{mn0} modes * cannot exist in cavities, with or without plasma.

* The notation m, n, p (here $p = 0$) characterizes respectively, the two transverse (here azimuthal and radial), and the axial mode modulations.

The homogeneous conditions of the type (52) cannot hold everywhere on the conductive enclosure of the plasma for the necessity to feed in the microwave power. The efffect is that (a) there will be a certain field configuration *imposed* at the feed point in the wall which usually leads to selective mode excitation. Locally, (b) the *induced* field will possibly be distorted, because the nodal plane formed by the wall is interrupted there. The latter effect can be minimized by an appropriate feed geometry, while the first underscores the necessity to know *all* field components from Sect. II.C in order to know which mode is being excited, in particular for nearly degenerate modes with only slightly different resonance frequencies (Sect. II.E.3-5).

E. Examples of Diagnostic Interest

1. Free Propagation in a Magnetized Plasma: Microwave Interferometry

We shall consider now a typical configuration, used in interferometry in a magnetized plasma column of large diameter (compared with the probing wavelength). From Fig. 2 it is clear that a magnetic field even for $\omega_c > \omega_p$ has essentially no effect on the dielectric tensor, and therefore on the microwave propagation for $\omega \gg \omega_{\text{hybrid}} = \sqrt{\omega_c^2 + \omega_p^2}$, for which we have $D \to 0, S \to P \to 1$. But this also implies that the plasma density must go to zero, a case that is not desirable for a density measurement. To extend the useful range, even in the presence of a magnetic field, the geometry schematically shown in Fig. 4 is employed: A waveguide carrying a probing microwave power in TE_{10} mode is expanded into a horn. As a result, the emerging wave vector is largely parallel to the waveguide (Fig. 4(a)). The waveguide with horn antenna is pointed at the plasma, oriented such that the wave's electric field vector is parallel to the static magnetic field $\vec{\mathbf{B}}_o$ that is embedded in the plasma (Fig. 4(b)). The wave vector component along $\vec{\mathbf{B}}_o$ vanishes approximately (i.e., $k \to 0$), and the wave will propagate *inside the plasma* as a pure TE mode with a wave vector, say, k_x. From Eqs. (22) and (23) we see that then

$$(k_x^2 - k_o^2 P) E_z = 0 \tag{54}$$

$$B_z \to 0 \tag{55}$$

Inserting this into Eqs. (34), (35) or (37) we conclude that $B_L = -B_R = ik_x E_z/\sqrt{2}$,

i.e., $B_x \to 0, B_y = -k_x E_z$. The characteristic wave propagation, or dispersion follows from condition (54) for non-trivial E_z:

$$k_x^2 = k_o^2 P = \mu_o \epsilon_o (\omega^2 - \frac{\omega_p^2}{1 - \frac{i\nu}{\omega}}). \tag{56}$$

As already discussed in Sect. II.A, whenever $n_e > n_c$ (disregarding ν at this point), the wave cannot propagate. Then, namely, $k_x^2 < 0$, resulting in solutions that spatially decay exponentially in the x-direction. Otherwise, measuring the wavelength *in the plasma*, $\lambda_p = 2\pi/k_x$, the electron density n_e can be determined via the plasma frequency (6).

As simple as the above derivation is, it forms the basis of any microwave interferometry used to determine the plasma density. It is valid under the assumption that (a) the plasma diameter be large, i.e., many plasma wavelength across, and (b) that there be no sizable diffractive plasma effects that could deflect the wave from its direction of propagation. Both assumptions can become violated when $n \to n_c$, since then, from Eq. (56), $k_x \to 0$, or $\lambda_p \to \infty$, a reason why we have always stressed the wavelength *in plasma*. We shall discuss these questions briefly in Sec. II.F, while all aspects of interferometry will be covered in Sec. IV.

2. Free Propagation in a Magnetized Plasma: Faraday Rotation

We now consider a plane wave travelling *along* the magnetic field, and assume no boundaries nearby. From Eq. (26) we see that a left-polarized and a right-polarized wave each travels with different speed. Consequently, the polarization vector of a linearly polarized microwave will rotate along the magnetic field direction. This Faraday-rotation effect is used to measure the line integrated density along the field lines, supposing that the magnetic field strength is known. For simplicity we disregard any collisionality effects. From Eq. (26), the angle of rotation γ, that results for propagation through an axial distance z_o is given by

$$\gamma = 2\pi \frac{z_o}{\lambda_o} [\sqrt{1 - \frac{\omega_p^2}{\omega(\omega + \omega_c)}} - \sqrt{1 - \frac{\omega_p^2}{\omega(\omega - \omega_c)}}]. \tag{57}$$

The vacuum wavelength of the microwave radiation was denoted by λ_o. For low densities where $\omega_p \ll \omega$, the term in the brackets can be approximated by $[\ ] \approx \omega_p^2 \omega_c / \omega(\omega^2 - \omega_c^2)$,

making γ proportional to the electron density n_e [c.f. Eq. (6)]. A more detailed account of the Faraday effect in plasmas and of the suitable microwave diagnostic techniques are given by Künstler (1965).

3. Cavity Resonances: The Unmagnetized Homogeneous Plasma

To gain some insight in resonances in plasma filled cavities, and the accompanying mode structures, we treat in this section the simplest possible case, where the *unmagnetized* plasma fills the cavity entirely. Then, and only then, by the arguments given in Sects. II.C.1 and II.D, pure TE and TM modes exist, as they are familiar from empty cavities (Gandhi, 1981). All the equations for the plasma-filled cavity reduce here to the equations governing the modes in an empty cavity, only that the following substitution is to be made:

$$\epsilon_o \rightarrow \epsilon_o P \tag{58}$$

Mode structures and resonance frequencies of empty cavities of various cross sections and configurations can be found in the microwave literature. As a specific example, we choose the frequently used TM_{0n0} modes in a cylindrical cavity of radius r_c, for which $k = m = 0$. There the resonance frequency is given by the condition [c.f. Eq. (22)]:

$$J_o(\kappa_E r_c) = J_o(\omega\sqrt{\mu_o\epsilon_o P(\omega)}r_c) = 0. \tag{59}$$

Specifically, the mode with no radial nodes, labeled by $n = 1$, that arises from the first zero of Eq. (59), displays the resonance frequency, disregarding collisional effects, by virtue of Eq. (10)

$$f_{010} = \frac{\omega_{010}}{2\pi} = \frac{1}{2\pi}\sqrt{\frac{2.405^2 + n_e e^2 \mu_o r_c^2/m}{\epsilon_o \mu_o r_c^2}}, \tag{60}$$

from which the electron density n_e can be extracted.

4. Cavity Resonances: The Unmagnetized Inhomogeneous Plasma

Everywhere up to this point in Sect. II, we have dealt with a homogeneous plasma, whose properties, as they enter the dielectric tensor, are spatially constant. In order to get an impression of how much any spatial variation of $\overleftrightarrow{\epsilon}$ may influence the resonance

frequency, we also give now the equations for an isotropic, non-magnetized, but inhomogeneous plasma, as they can be derived from Maxwell's equations (13) to (16):

$$\nabla^2\vec{\mathbf{E}} + k_o^2\epsilon(\vec{\mathbf{r}})\vec{\mathbf{E}} + \nabla(\vec{\mathbf{E}}\cdot\nabla)ln\epsilon(\vec{\mathbf{r}}) = 0 \tag{61}$$

and

$$\nabla^2\vec{\mathbf{B}} + k_o^2\epsilon(\vec{\mathbf{r}})\vec{\mathbf{B}} - (\nabla\times\vec{\mathbf{B}})\times\nabla ln\epsilon(\vec{\mathbf{r}}) = 0 \tag{62}$$

The analysis of these equations becomes rather simple for the case where (a) the fields have no axial or azimuthal dependence (i.e., $k = m = 0$), * and (b) the dielectric constant depends solely on $r, \epsilon = \epsilon(r)$. For comparison with the TM_{0n0} modes discussed in Sect. II.E.3, Eqs. (61) and (62) reduce, with $\vec{\mathbf{E}} = E\hat{\mathbf{e}}_z, \vec{\mathbf{B}} = B\hat{\mathbf{e}}_\varphi$, to

$$(\nabla_\perp^2 + k_o^2\epsilon(r))E = 0 \tag{63}$$

$$(\nabla_\perp^2 + k_o^2\epsilon(r))B - i\omega E\frac{\partial\epsilon(r)}{\partial r} = 0. \tag{64}$$

If we assume that the plasma is in contact with the wall, we can immediately find the resonance condition by imposing the radial boundary condition (52) upon E at $r = r_c$. For this, it sufficient to seek solutions only to Eq. (63), as it does not depend on B, and B does not enter the boundary conditions (52).

For a parabolic plasma density profile, we have

$$n_e(r) = \hat{n}(1 - \delta\frac{r^2}{r_c^2}), \quad \text{or} \quad \epsilon(r) = \epsilon_1 + \epsilon_2\frac{r^2}{r_c^2}, \tag{65}$$

where

$$\epsilon_1 = 1 - \frac{\hat{\omega}_p^2}{\omega(\omega - i\nu)}; \quad \epsilon_2 = \delta\frac{\hat{\omega}_p^2}{\omega(\omega - i\nu)}; \quad \hat{\omega}_p = \omega_p(n_e \to \hat{n}). \tag{66}$$

The quantities $\hat{n}$ and δ follow from Fig. 5(a), and are entirely arbitrary, although a physically reasonable choice would assume $\hat{n} < n_c$, $0 < \delta < 1$. Using the abbreviation

* Another reason to consider only modes with $k = m = 0$ is that otherwise no pure TM or TE modes can exist for a radially varying plasma, as discussed in Sect. II.D. This of course would also follow directly from Eqs. (61) and (62).

$\hat{k}_o^2 = \hat{\omega}_p^2 \mu_o \epsilon_o \delta / r_c^2$ the solution

$$\vec{\mathbf{E}}(r) = \hat{\mathbf{e}}_z E_o \mathrm{Re}\ e^{\pm i r^2 \hat{k}_o}\, {}_1F_1[\frac{1}{2}(1 \mp i\epsilon_1 k_o^2/\hat{k}_o), 1, \mp i r^2 \hat{k}_o] \tag{67}$$

can be written in terms of confluent hypergeometric functions. Since their zeros are somewhat awkward to discuss, we choose a slightly different power-law profile. This will permit to make a direct comparison with the results of the preceding section, to estimate the effect of the density profile on the TM_{0n0} resonance frequency. We assume the worst possible case, where the density on axis $\hat{n}$, takes the critical value n_c from Eq. (11), for which $\epsilon_1 = 0$. * Clearly, for a rectangular profile, as assumed elsewhere in Sect. II, no oscillatory fields could form in the cavity for $\epsilon = 0$. Therefore, to determine the influence of the profiles we will instead require that the radially integrated density $\int r dr n_e(r)$ be the same for the rectangular and the power law profile defined by

$$n_e(r) = n_c[1 - \delta(\frac{r}{r_c})^{2\lambda}], \quad \text{or} \quad \epsilon(r) = \delta(\frac{r}{r_c})^{2\lambda}. \tag{68}$$

Again δ and $\lambda \geq 0$ are arbitrary (c.f., Fig. 5(b)). The equivalent mean density is then $\bar{n} = n_c[1 - \delta/(\lambda + 1)]$. The solution for a profile of the form (68), takes the form

$$\vec{\mathbf{E}}(r) = \hat{\mathbf{e}}_z E_o J_o(\omega \sqrt{\mu_0 \epsilon_o \delta} \frac{r_c}{(\lambda + 1)} (\frac{r}{r_c})^{\lambda+1}) \tag{69}$$

The ratio of the resonance frequencies for the rectangular profile of Sect. II.E.3 and of the power-law profile (68), with the same mean density,

$$\frac{\omega^r}{\omega^p} = \sqrt{1 - \frac{\lambda\delta}{(\lambda + 1)^2}} \tag{70}$$

is rather insensitive to the choice of δ and λ, where $0 \leq \delta \leq 1$, and $\lambda > 1/2$. Consequently, the error in the density determination, incurred by assuming a rectangular rather than a diffused profile is, at least for the TM_{0n0} modes, small.

---

* Because of the nonlinear (square-root type) dependency of the resonance frequency on P, and therefore on n_e [c.f., Eqs. (59) and (60)], the profile properties will play their greatest role for $\hat{n} \to n_c$.

5. The General Cavity Resonance Condition: The Homogeneous Plasma Column

After having discussed the resonance conditions for an unmagnetized plasma, both homogeneous and inhomogeneous, that fills entirely a cylindrical cavity, we will now consider the general situation: A circular magnetized, homogeneous plasma column of radius r_o is coaxially situated in a cylindrical waveguide or cavity. Again, we will not concern ourselves whether there are axially standing or running waves, that differentiate the two applications under the following proviso: In addition to the critical condition given below, the cavity case will require that the axial wavelength $\lambda = 2\pi/k$, be determined by the length of the cavity, l_c, via

$$k = \frac{p\pi}{l_c}, \tag{71}$$

in order to match the axial boundary conditions, with the exception of the TM_{0n0} family, where all the field components that are subject to these axial conditions, vanish identically.

Recalling the host of wave solutions and boundary conditions, and in particular the fact, that, for $k \neq 0$, no pure TE or TM modes can exist, it may appear at first glance a hopeless venture to treat the general case. However, all that is needed in order to find the specific solutions and the corresponding set of critical conditions is that the 6×6 coefficient determinant vanish. The six homogeneous equations, or the matrix of coefficients, for the six independent unknowns of Eqs. (28), (29), (39), (40), (45), (46) and (47), here chosen to be $\mathcal{E}_1, \mathcal{H}_2, \mathcal{F}_1, \mathcal{F}_2, \mathcal{G}_1$ and $\mathcal{G}_2$, can be composed in the compact scheme of Table I. The omitted arguments of the functions $\mathcal{A}_i$ and $\mathcal{B}_i$ [c.f. Eqs. (41) and (42)], e and h [c.f. Eqs. (32) and (33)], and $\mathcal{K}_j^i$ [c.f. Eq. (48)] follow from their respective rows and columns. The empty squares are meant to be zero. As an example, the equation for $E_z(r_o)$ (first row) would thus read:

$$J_m(\kappa_1 r_o)\mathcal{E}_1 - J_m(\kappa_v r_o)\mathcal{F}_1 - Y_m(\kappa_v r_o)\mathcal{F}_2 + e(\kappa_2)J_m(\kappa_2 r_o)\mathcal{H}_2 = 0 \tag{72}$$

As in the two preceding sections, an infinite set of characteristic solutions will ensue because of the multi-valuedness of the principal solutions, i.e., here the Bessel functions. For $k \to 0$ and $m \to 0$, a case that was discussed in detail by Buchsbaum *et al.* (1960), we

see, in light of the limit values of $\mathcal{A}, \mathcal{B}, e$ and h that the 6×6 matrix of Table I becomes reducible into two 3×3 matrices. Hence, pure TM modes (where $\mathcal{H}_2 = \mathcal{G}_1 = \mathcal{G}_2 \equiv 0$), or pure TE modes (where $\mathcal{E}_1 = \mathcal{F}_1 = \mathcal{F}_2 \equiv 0$) are then permitted, regardless of whether the plasma is magnetized or not. But while TM_{0n0} modes can exist in an axially bounded cavity, the TE_{0n0} modes exist only as cutoff modes TE_{0n} in a waveguide. The electrostatic limit for which $\omega \to 0$, yields similarly a reducible blockform, which is most easily seen when the rows for $E_\varphi(r_o)$ and $H_\varphi(r_o)$ are interchanged.

Finally, for comparison with the TM_{0n0} mode family in an unmagnetized plasma, discussed in the two preceding sections, we consider the simpler case resulting from Table I, when the plasma fills the cavity completely ($r_o = r_c$). The subset of conditions from Table I is then

$$J_m(\kappa_1 r_c)[k\mathcal{A}_2(\kappa_2, r_c)e(\kappa_2) - \omega\mu_o\mathcal{A}_1(\kappa_2, r_c) = e(\kappa_2)J_m(\kappa_2 r_c)\times \\ [k\mathcal{A}_2(\kappa_1, r_c) - \omega\mu_o\mathcal{A}_1(\kappa_1, r_c)h(\kappa_1)]. \tag{73}$$

Particularly, for $k = 0, m = 0$, and by virtue of Eqs. (25), (32), (33), (43) and (44), this reduces to

$$J_o(\kappa_E r_c)J_1(\kappa_H r_c) = 0, \tag{74}$$

permitting either $\mathcal{E}_1 \equiv 0$ for $J_1(\kappa_H r_c) = 0$, or $\mathcal{H}_2 \equiv 0$ for $J_o(\kappa_E r_c) = 0$. The latter is, as above, the condition for the TM_{0n0} cavity modes where, as in the unmagnetized case Eq. (58), the substitution

$$\epsilon_o \to \epsilon_o P \tag{75}$$

makes the connection to the empty-waveguide or cavity solution. The second condition can only be fulfilled for a TE_{0n} waveguide mode at cutoff.

In section III.B.1, we present approximate perturbation techniques to simplify the results of the present section. They may be used whenever the plasma introduces a small perturbation to the fields of a cavity, either by a low plasma density, or by a thin plasma column, $r_o \ll r_c$.

F. Optical Approximations: Diagnostic Applications

Starting from Maxwell's equations as they apply to dielectric media, light refraction and diffraction can be suitably described by *geometric optics* or by *wave optics.* Both deal with the modification of the light propagation by the dielectric properties of matter, and its boundary surfaces. Wave optics are appropiate whenever the wavelength is of the same order of the magnitude as the characteristic dimensions of the dielectric body, and plane waves are a reasonable assumption. Geometric optics are applicable when the wavelength is much smaller than any characteristic gradient length (Cornbleet, 1976 and 1984). Given the appropriate range of validity, the same formulations may be applied to microwave propagation. They yield efficient tools for a qualitative, and, often times, excellent quantitative description of the propagation phenomena. Microwave lenses and mirrors, but also beam refraction or deflection by plasma density gradients are common examples for the use of geometric optics. On the other hand, diffraction patterns emerging from horn antennae, the Fabry-Perot transmission and reflection properties of a plasma layer, or the coherent Bragg scattering of microwaves off a plasma density wave are well described by wave optics.

Rather than justifying the theoretical basis of these optical approximations, which can be found in an abundant literature (Cornbleet, 1976 and 1984) we will only briefly cite a few applications useful to the diagnostician.

1. Microwave Horn Antennae and Microwave Imaging

While microwave power is best transported in waveguides, it is frequently necessary to shine it into a plasma sample for investigation. For this, horn antennae are used (Love, 1976; Milligan, 1985). Lenses and mirrors are employed when better imaging is necessary, for instance for improved spatial resolution (Primich *et al.*, 1965). Microwave lenses are usually made from a polymeric compound of suitable refractive index (Brown, 1953; Gandhi, 1981; Milligan and McDonnell, 1986). Another possibility for a lens is to use a plano-concave metallic channel plate, which, via Huygens' principle, transforms, say, a spherical wavefront into a plane wave front, and vice versa (Uckan 1981). Mirrors serve not only for imaging purposes, but also for double path transmission of interferometric

measurements in low-reflection plasmas (Efthimion, et al., 1985; Overzet and Verdeyen, 1986); and mitre box type mirrors are, for example, used for microwave beam scanning applications (Uckan 1983). Partially reflecting mirrors and grid polarizers permit experimental setups essentially equivalent to their counterparts in light optics (Fellers, 1962; Davis and Patsakos, 1983; Suvorov *et al.*, 1984).

2. Optical Refraction in Plasma Columns

Associated with the dielectric constant of a plasma there is also a refractive index defined by

$$n_r = \frac{c}{v_{\text{phase}}} = \frac{kc}{\omega} = \frac{k}{k_o} \tag{76}$$

In the geometry of Sect. II.E.1, this becomes using Eqs. (54), (55) and (10)

$$n_r = \sqrt{P} = \sqrt{1 - \frac{\omega_p^2}{\omega(\omega - i\nu)}}. \tag{77}$$

As long as $\nu \ll \omega$, the effective refractive index of a plasma is $n_r < 1$, unlike in most other optical materials. With the identification (77), we can characterize the refractive imaging properties of a homogeneous plasma column in analogy to the optics of a cylinder lens (Meuth, 1986). This simple calculation is usually sufficient to estimate the deflection that the beam may suffer in multi-channel or scanning microwave interferometers, or the divergence in transmission measurements. For inhomogeneous plasmas of circular or elliptic cross section, the more realistic, but also more involved ray-tracing method is available, based on Eqs. (54) or (63) (Shmoys, 1961; Jones and Wooding, 1965; Faugeras, 1965; Tallents, 1984), see also Sec. IV.D.1.

3. Fabry-Perot Methods

Similar to the resonances in cavities, and the propagation characteristics in waveguides, whereby the electromagnetic waves bounce back and forth, reinforcing themselves constructively, there are such resonance and transmission phenomena in any bounded dielectric, be it enclosed by a metal wall, another dielectric or by vacuum. Dielectric waveguides are an example; when immersed into a plasma, the altered wave propagation in

the waveguide can be used to determine the plasma density interferometrically with high spatial resolution (Stewart and Robson, 1965; Lisitskaya and Shustin, 1981; Armand *et al.*, 1982).

As in the case of an optical interference filter, a plasma slab or column displays transmission and reflection characteristics for microwave radiation near the cutoff, that are oscillatory with frequency, or plasma density. This effect is due to multiple internal reflections in the plasma (Heald and Wharton, 1978). With the plasma density approaching its critical value given by Eq. (11), the wavelength *in the plasma* becomes large according to Eq. (56). Hence, the situation where the wavelength is of the order of the plasma slab thickness or column radius, may easily arise. Moreover, if the plasma is situated in a conductive chamber, microwave reflections off nearby walls can make a similar additional effect, making the interpretation of measurements difficult. This is of particular importance, when the plasma density and therefore the plasma wavelength vary with time. The Fabry-Perot effect can be exploited to reduce such unwanted reflections from metallic walls by methods similar to those used for anti-reflection coatings in optics (Severin, 1956; Kato and Hutchinson, 1984). The most desirable situation, especially for microwave interferometry, is that the plasma density be low, while its thickness accomodate many wavelengths. However, this cannot always be achieved. For higher plasma densities, $n_e \rightarrow n_c$, and smaller column width, $\lambda \sim r_o$, a Fabry-Perot cell, in conjunction with focussing lenses, can be employed (Bize *et al.*, 1965; Primich *et al.*, 1965; Davis and Patsakos, 1983).

III. CAVITY AND WAVEGUIDE DIAGNOSTIC TECHNIQUES

In Sec. II.E, the propagation and resonance conditions for microwaves in bounded and unbounded plasmas were derived. We now proceed to various experimental schemes to measure such propagation or resonance properties for plasmas in waveguides or cavities. The final goal is, as already mentioned, to determine the plasma parameters, as density, collisionality, and, in some instances, also the electron temperature.

A. Cavity and Waveguide Loading by a Plasma

A cavity resonance can directly be observed by insertion of a small probe (Sec. III.B).

The presence of a plasma in a waveguide or a cavity can be measured by the microwave transmission, absorption, or reflection that the plasma causes. In any case, the plasma can be interpreted as a load. We include both a *dissipative* load, that converts electromagnetic energy into thermal energy and a *reactive* load, that, like in an inductor or a capacitor, only temporarily stores energy, usually in an oscillatory fashion, cycling energy into and out of the rest of the microwave circuit. Once the notion of a load (or impedance) is in hand, the reduction to a lumped circuit scheme is simpler (Adler *et al.*, 1960; Fano *et al.*, 1960). Therefore, we first determine the flow of energy in and out of a plasma-cavity or waveguide configuration.

1. Poynting's Theorem

The energy associated with the wave fields follows from Maxwell's equations (13) and (15):

$$\frac{1}{2}\frac{\partial(\epsilon_o E^2 + \mu_o H^2)}{\partial t} + \nabla \cdot (\vec{\mathbf{E}} \times \vec{\mathbf{H}}) = -\vec{\mathbf{j}} \cdot \vec{\mathbf{E}}. \tag{78}$$

The Poynting's theorem (78) is nothing else than the continuity equation for the energy density of the electromagnetic fields, $u = \epsilon_o E^2/2 + \mu_o H^2/2$; its changes are due to energy convection, given by the poynting vector $\vec{\mathbf{E}} \times \vec{\mathbf{H}}$, or due to the work done by the electric field on all the charged particles, and vice versa. The latter can be seen when equating $\vec{\mathbf{j}} \cdot \vec{\mathbf{E}} = n\vec{\mathbf{F}} \cdot d\vec{\mathbf{x}}/dt = ne\vec{\mathbf{E}} \cdot d\vec{\mathbf{x}}/dt$. For the spatial and temporal field oscillations (20) or (21)where the Fourier amplitudes are still complex, Eqs. (13) and (15) lead to a somewhat different form:

$$i\omega(\epsilon_o|E|^2 - \mu_o|H|^2) = \nabla \cdot (\vec{\mathbf{E}} \times \vec{\mathbf{H}}^*) + \vec{\mathbf{j}}^* \cdot \vec{\mathbf{E}}. \tag{79}$$

Equation (78) is equivalent to (79), once it is integrated over one temporal or spatial period. Equation (79) provides a direct interpretation: (1) Magnetic and electric energy are 180° out of phase. (2) The *real part* of its RHS accounts for, as expected, a damping, or a dissipative load while the *imaginary part* gives rise to a reactance. In light of the complex conductivity (5), that enters, via Eq. (3), the term $\vec{\mathbf{j}}^* \cdot \vec{\mathbf{E}}$, the latter is of importance for plasmas with low collisionality. The complex conductivity is a consequence of the fact

that the plasma electrons can pick up and return field energy. They generate displacement currents, while their collisions lead to dissipation of the microwave power.

2. The Quality Factor or Q Value

In Sect. II.E, we saw that a plasma situated in a cavity will alter its resonance frequency and mode spectrum. Before discussing the diagnostic applications of this fact, we will first consider the resonance properties of a cavity. These may be characterized by the quality factor Q, defined as the ratio of the (energy stored in the cavity) $\times$ (resonance frequency, when no damping is assumed) to the average dissipated power *loss*. In order to compute these quantities, Poynting's theorem (78) is integrated over the cavity volume to get

$$\frac{1}{Q} = \frac{1}{\omega_o} \frac{\int dV \vec{\mathbf{j}} \cdot \vec{\mathbf{E}} + \int da \hat{\mathbf{n}} \cdot (\vec{\mathbf{E}} \times \vec{\mathbf{H}})}{\mu_o \int dV H^2}, \tag{80}$$

where, in the denominator, the fact was used that at resonance $\omega = \omega_o$, and after period averaging, electric-field energy = magnetic-field energy = 1/2 total electromagnetic energy. Note that, had Eq. (79) been used instead of Eq. (78), the Q value would then be defined as the *real part* of the resulting complex products analogous to those of Eq. (80), relating Q to the dissipation. * Clearly, for an *empty* cavity, whose walls have infinite conductivity, $Q \to \infty$, invoking the idealized conditions (50) and (52). For the realistic case of a very large, but finite wall conductivity σ_c (Jackson, 1975; Gandhi, 1981), the average power loss in the numerator of the RHS of Eq. (80) becomes, to leading order of $1/\sigma_c$, $\frac{1}{4}\mu_o \omega \delta H_{\|}^2$, where $H_{\|}$ is the magnetic field just outside the conductor, tangent to the cavity wall, and δ is the skin depth, $\delta^2 = 2/(\mu_o \omega \sigma_c)$. The field $H_{\|}$ follows from a mode calculation similar to the one presented in Sec. II, where the boundary conditions (50) and (52) remain, again to leading order in $1/\sigma_c$, *unaltered*. This implies that Q depends on the chosen mode. There are various simplifications possible for specific modes, e.g., the TM modes, and the Q factor can commonly be reduced to the form (Jackson, 1975),

$$Q = \left(\frac{V_c}{S_c \delta}\right) \times (Geometrical\ factor), \tag{81}$$

* Sometimes, the term Q *value* is also used for a cavity with a dielectric plasma present, which makes Q complex.

with V_c/S_c being the cavity's volume to surface ratio. The importance of the quality factor to the resonance width will be illustrated in the following section. The Q value *in the presence of plasma* follows also from Eq. (80), by inserting the fields, and the plasma conductivity discussed in Sec. II. Specifically, plasma effects will contribute to the Q value, if there are ohmic losses in the plasma, or if the wave fields are evanescent inside the plasma, which happens for $\omega < \omega_p$.

3. The Lumped Circuit Analog

The discussion of the preceding section can be illustrated for an LRC-circuit. There, the magnetic energy (in the inductor L) is $W_m = \frac{1}{2}LI^2$, I being the current, while the electric energy (in the capacitor C) is $W_e = \frac{1}{2}q^2/C$, q being the charge, with $\frac{dq}{dt} = I$ according to Kirchhoff's law. The power dissipated by the resistor R is given by Joule's heat, $P_t = RI^2$. Thus, conservation of energy (or Poynting's theorem) requires $\partial_t(W_m + W_e) = -P_t$. Consequently, the current I obeys the equation for *free* oscillations

$$L\frac{d^2I(t)}{dt^2} + R\frac{dI(t)}{dt} + \frac{I(t)}{C} = 0, \tag{82}$$

which, with $I(t) \propto e^{i\Omega t}$, gives

$$\frac{\Omega}{\omega_o} = \frac{i}{2Q} \pm \sqrt{1 - (\frac{1}{2Q})^2}. \tag{83}$$

The lossless resonance frequency is denoted by $\omega_o = 1/\sqrt{LC}$, whence the quality factor $Q = 2\omega_o W_m/P_t = \omega_o L/R$, using $W_m = W_e$ for $\omega = \omega_o$. Equation (83) can be solved for $1/Q$ to yield:

$$i(\frac{\Omega}{\omega_o} - \frac{\omega_o}{\Omega}) + \frac{1}{Q} = 0. \tag{84}$$

Meanwhile, for oscillations *forced* by an in-series drive, the RHS of Eq. (82) becomes $\partial_t u(t)$. With $u = u_o e^{i\omega t}$, the (stationary) solution for the current is then

$$I(t) = \frac{u_o}{\omega_o L}[\frac{1}{Q} + i(\frac{\omega}{\omega_o} - \frac{\omega_o}{\omega})]^{-1} e^{i\omega t}. \tag{85}$$

Writing I in terms of amplitude and phase $\mid I \mid e^{i\Phi(I,u)}$, the amplitude attains its largest (resonant) value for $\omega = \pm\omega_o$, and drops to one half of that for $|\omega/\omega_o| =$

$\sqrt{1+3/(2Q)^2} \pm \sqrt{3}/2Q$, in contrast with Eq. (83). And while current and voltage are in phase for $\omega = \omega_o$, the current *lags* the voltage, and vice versa, respectively, for $\omega > \omega_o$ (due mainly to the inductor), and for $\omega < \omega_o$ (due mainly to the capacitor). A totally different situation arises if the circuit is driven in *parallel.*

These examples show that, while the quality factor Q is directly related to a circuit's dissipation, the resonant properties, like resonance frequency and half width, depend, aside from Q, also on *how the currents* are permitted to *flow.* In a cavity, this is dependent upon the choice of mode, as already mentioned. Hence, a lumped circuit has to be chosen in accordance with a certain mode or mode family.

Lumped circuits provide not only model descriptions for resonant cavities, but also for the mentioned transmission, reflection and absorption measurements usually far away from any resonance. Terms as impedance, with its real part, the resistance, and its imaginary part, the reactance, (or, inversely, the admittance, with conductance and susceptance, respectively), have all their counterpart for waveguides, and can be calculated from the wave fields via Poynting's theorem (78) or (79) (Adler *et al.*, 1960; Fano *et al.*, 1960; Jackson, 1975).

B. Resonant Cavity Techniques

One of the earliest plasma diagnostic techniques, the resonant cavity method was developed by Slater (1946), and first applied to the characterization of ambipolar diffusion in a helium plasma (Biondi and Brown, 1949). As already mentioned, the presence of the plasma in the cavity will result in both a shift of the cavity's resonance frequency and a change in the Q value. These two effects are, respectively, related to the plasma frequency, and therewith the electron density, and to the frequency of collisions of the electrons with other plasma or neutral particles. The early success of this technique was based on the fact that the experimental results had a simple theoretical interpretation, when employing a first order perturbation theory, which obviated a machine computation, something rather involved in those days. However, in order for the perturbation approach to be valid, a series of conditions on configuration and parameters of the plasma have to

hold, which cannot always be met under laboratory conditions (Chen *et al.*, 1968). The rigorous, in the limit of a homogeneous cold plasma model, methods of Sec. II must then be employed to compute the resonance frequencies and the mode structures in a cavity, and its dependence on the plasma density, collision frequency, plasma radius and the physical dimensions of the cavity.

1. Perturbation Theory Formulae

The assumption is made that the plasma, or the displacement currents in the plasma modify only very little the resonant wave fields of an empty cavity. Following Slater (1946), we describe the damped cavity oscillations, just as in Sec. III.A.3, by means of the real and imaginary part of the angular frequency ω, as given by Eq. (79). There, the energy flow in and out of the interior of the *cavity* is determined by $\nabla \cdot (\vec{\mathbf{E}} \times \vec{\mathbf{H}}^*)$, the imaginary part of which accounts for the wave reflections off the walls, and thus gives rise to the cavity resonance frequency, while its real part accounts for dissipation in the wall, leading to damping, characterized by Q. Assuming that the currents $\vec{\mathbf{j}} = \overleftrightarrow{\sigma}\vec{\mathbf{E}}$, in the *plasma* are mainly non-dissipative displacement currents, $\nu \ll \omega_p$, we can obtain from Eq. (79) the small relative frequency shift due to the plasma (Biondi and Brown, 1949; Biondi, 1951; Buchsbaum, *et al.*, 1960):

$$\frac{\delta\omega}{\omega} = -\frac{1}{2\omega\epsilon_o}\frac{\mathrm{Im}\int dV \vec{\mathbf{E}}^* \cdot \overleftrightarrow{\sigma}\vec{\mathbf{E}}}{\int dV |E|^2}. \tag{86}$$

The complex conductivity tensor $\overleftrightarrow{\sigma}$ is given by Eqs. (5), or (8) and (9), and the integration is to be taken over the cavity volume; the resonant frequency ω, and the wave fields $\vec{\mathbf{E}}$ are those for the empty cavity. When dealing with a non-magnetized plasma, where σ is a scalar, Eq. (86) reduces further to

$$\frac{\delta\omega}{\omega} = -\frac{1}{2\omega\epsilon_o}\frac{\int dV \mathrm{Im}\sigma |E|^2}{\int dV |E|^2} = -\frac{\bar{n}e^2}{m\omega^2\epsilon_o}G. \tag{87}$$

From the discussions in Sec. II, this result also applies to magnetized plasmas, when a TM_{0m0} cavity mode is used. Thus, aside from a yet to be determined geometrical factor G, the average plasma density $\bar{n}$ can directly be inferred from measuring the relative resonance

frequency shift $\delta\omega/\omega$. Various authors have derived or used approximate formulae for G (Biondi 1951; Buchsbaum *et al.*, 1960; Golant, 1960; Anissimov *et al.*, 1965; Bisschops and de Hoog, 1985), defined in terms of the known, unperturbed electric field distribution $\vec{\mathbf{E}}(\vec{\mathbf{r}})$ and the *assumed*, or determined by other diagnostic measurements, density distribution $n(\vec{\mathbf{r}})/\bar{n}$:

$$G = \frac{\int dV |\vec{\mathbf{E}}(\vec{\mathbf{r}})|^2 n(\vec{\mathbf{r}})/\bar{n}}{\int dV |\vec{\mathbf{E}}(\vec{\mathbf{r}})|^2}, \tag{88}$$

and a similar, although somewhat more complicated definition holds, if $\overleftrightarrow{\sigma}$ is still a tensor. Therefore, unlike in the rigorous model description of Sec. II, plasmas with an *axial density variation* may be described by the perturbation approximation, as long as the latter is justified.

A perturbation approximation is usually applicable when the plasma modifies but little the empty cavity fields. This is the case whenever (a) $\omega_p \ll \omega$, $\nu \ll \omega$, and (b) if a magnetic field is used, for $\omega_c \ll \omega$, or (c) the radius of the plasma column, r_o, is much smaller than the cavity radius, r_c *irrespective of how large the plasma density*, as long as the penetration depth ε for the evanescent cavity fields $\varepsilon \gg r_o$. The depth ε is, in the absence of collisions, not related to the skin depth used in Sec. III.A.2, but is of the order of (Buchsbaum *et al.*, 1960):

$$\varepsilon \sim \frac{c}{\omega} \frac{1}{\sqrt{\frac{\omega_p^2}{\omega^2} - 1}}. \tag{89}$$

As an example, we evaluate Eq. (86) or (87) for the TM_{010} mode. The electric field is then $E_z \propto J_o(r\omega/c)$ (Gandhi, 1981; Secs. II.C.2 and II.E.3), where $r_c\omega/c = 2.405$ in order to meet the radial boundary condition (49). Furthermore, since $k = m = 0$, $\overleftrightarrow{\sigma} \rightarrow \sigma_P$ [Eq. (5)], which is non-zero only within the plasma column, $r \leq r_o$. For $r_o \ll r_c$, the integral in the numerator may be expanded and evaluated by the mean-value theorem, to yield $(\bar{\omega}_p^2/\omega^2)(r_o^2/2)$, while the integral over the cavity radius in the denominator is evaluated by standard procedures for Bessel functions. As the final result we get the average electron density in terms of the frequency down shift $|\delta\omega|$, the resonant frequency ω, and the plasma

cavity radius, r_o and r_c:

$$\bar{n}_e = 0.54\frac{\epsilon_o m}{e^2}\omega|\delta\omega|\frac{r_o^2}{r_c^2}, \tag{90}$$

or, with $\omega = 2\pi f$ (Hz):

$$\bar{n}_e = 6.7 \times 10^{-3} f|\delta f|\frac{r_o^2}{r_c^2} \quad (\mathrm{m}^{-3}). \tag{91}$$

Whenever the above mentioned conditions for a perturbation approximation apply, then the *quantitative* range of validity of Eqs. (86) through (88) can be determined by appropiate Taylor expansions of the general resonance condition of Sec. II.E.5 (for specific examples see Buchsbaum *et al.*, 1960; Agdur and Enander, 1962; Lieberman and Lichtenberg, 1969). This procedure is only correct in the absence of axial density gradients. For plasmas with such gradients, only qualitative arguments can be given, usually invoking the electrostatic approximation which is generally not valid. In such a case, the validity limits cannot be quantified, potentially giving rise to an appreciable systematic error when interpreting resonant cavity measurements by means of Eq. (86) or (87).

2. Cavity Configurations and Microwave Circuitry

A number of cavity configurations are commonly in use, generally in the shape of a right circular cylinder (Biondi, 1951), although rectangular cavities can be used (Schulz and Brown, 1955). Depending on the configuration and technique, the density range roughly suggests what microwave frequency to use. Frequencies between 1.5 and 10 GHz, and rarely, up to 35 GHz have been reported in the literature. Since the cavity has to be resonant at the chosen or available frequency and mode, this will determine the overall dimensions.

a) Empty Cavity. The resonance frequency of an empty cavity, for an (m, n, p) mode is given by

$$f_r = \frac{c}{2}\sqrt{\frac{\alpha_{mn}^2}{b^2} + \frac{p^2}{l}}. \tag{92}$$

The axial length of the cavity is denoted by l, while the parameter α_{mn} depends on the transverse geometry. For a rectangular resonator with major and minor dimensions a and b, $\alpha_{mn}^2 = m^2 + n^2 b^2/a^2$, for both TE and TM modes. For a circular cylindrical resonator

of radius $r_c = b$, $\pi\alpha_{mn}$ is the n^{th} zero of $J'_m(\pi\alpha_{mn}) = 0$ for TE modes; and the n^{th} zero of $J_m(\pi\alpha_{mn}) = 0$ for TM modes. If the transverse dimensions a, b or r_c are much smaller than the axial dimension l (or vice versa) the first (second) term under the square root in Eq. (92) becomes dominant, assuming a low order mode, where $\{m, n, p\} = \{0, 1, 2\}$. Thus for $r_c \ll l$, the resonance frequencies become virtually independent of the cavity length. This is always the case for the TM_{mn0} mode family.

b) Open Cavity. Open cavities (Fig. 6(a)), i.e. cavities with no axial end plates, are based on this fact. But at high wave numbers p (shorter axial wave number k), they behave more like waveguides. This type of cavity and its diagnostic applications are discussed by Vainstein (1963) and Anissimov, *et al.* (1965).

c) Closed Cavity. The most common type is the closed cavity. Two typical configurations are shown in Fig. 6(b) and (c). To interpret the measurement for high densities ($n > n_c$) by means of the perturbation theory of the preceding section, the radius of the non-conductive plasma vessel has to be much smaller than the cavity radius (Fig. 6(b)). This is also advisable to minimize the effect upon the Q value of the two holes in both end plates that serve as feed-throughs for the quartz tube. Circular waveguides, that are well below cutoff for the cavity resonance frequency, usually extend from these holes to reduce radiation losses. Choosing a thin-walled quartz tube minimizes its dielectric effect in the cavity. All these deviations from an ideal cavity may distort the fields near the holes (fringe fields). A change in Q and the resonance frequency, compared with their calculated ideal values, is the result; and a recalibration, possibly with a dielectric rod, instead of the plasma column, may be necessary (Chen *et al.*, 1968).

These problems can largely be avoided if the plasma vessel and the cavity are the same (Fig. 6(c)). Such a configuration requires that both the microwave power that *generates* the plasma, and the *probing* microwave radiation are fed into the same cavity, although each may form a different cavity mode (Schulz and Brown, 1955; Asmussen *et al.*, 1974). Frequently, plasmas are also generated by power application in the radio-frequency (rf) range, for instance in a plasma reactor with plane parallel electrodes. Both electrodes can

be configured such that they close to a microwave cavity (Bisschops and de Hoog, 1985), possibly using appropiate choke connections that are matched for the microwave frequency while constituting a high impedance for the rf frequencies in the MHz range. When using such a plasma vessel cavity configuration it is permissible to apply the perturbation formulae of Sec. B.1, only for low plasma densities, whenever $\omega_p \ll \omega$.

Most measurements in closed circular cylindrical cavities of either type of Fig. 6(b) or (c) are based on the TM_{0n0} mode family, usually for low order modes, $n = 1$, or 2. The reason for this is (c.f. Secs. II.E.3 to E.5) the simple interpretation of the results in this case, since such pure TM_{0n0} modes can exist in a cavity, be it empty, partially or entirely filled,with a plasma of arbitrary density or collisionality, and with or without an embedded axial magnetic field, that is present in many experimental configurations. The empty-cavity Q value for these modes is easily calculated (Sec. III.A.2), and the perturbation formulae become particularly simple (Sec. III.B.1). By choosing the dimensions such that $r_c/l > 0.493$ [c.f. Eq. (92)], the TM_{010} mode will have the lowest cavity resonance frequency, which can be helpful for unambiguous mode determination. The most commonly selected mode is the TM_{010} mode, although there are also benefits in choosing the TM_{020} mode instead (Harris and Balfour, 1965). Since the resonance frequency for any of the TM_{mn0} modes is independent of the cavily length l (since $k = p = 0$), the cavity lacks simple tunability for such modes. Modes with $p \neq 0$ can be tuned by means of sliding endplates (Asmussen *et al.*, 1974).

d) Large Plasma Vessel. Sometimes, the experimental or technical situation necessitates a rather large plasma vessel. It is simultaneously to be used as a cavity, high mode numbers m, n and p will be the consequence, whenever the dimensions a, b and l are much larger than the vacuum wavelength for the used microwave frequency. But as long as the quality factor of the vessel is sufficiently large, the density can still be determined by the plasma-induced frequency shift (Akulina, 1965; Fessenden and Smullin, 1965). A high cavity Q is required in order to separate well any of these high order modes that are narrowly spaced in frequency, and can be accomplished by low-resistance chamber-wall seams and joints, and a minimum of feed-through orifices.

e) Capacitor Resonator. Frequencies in the low microwave or the high rf range are used to excite dipole resonances in a plasma column, situated in a capacitor type resonator (Fig. 6(d)). Such a resonator is more akin to a TEM structure than a cavity. The dipole resonances are closely related to the plasma frequency (Tonks, 1931; Dattner, 1961), and can therefore also be used to measure the plasma density. For this low frequency range the electrostatic limit is invoked that suppresses all the rf magnetic fields in comparison with the electric fields. The employed diagnostic frequency must still be much higher than any characteristic ion frequency. The electrostatic potential obeys Laplace's equation. For a cylindrical plasma column of radius r_o, placed into a plane-parallel capacitor, with plate spacing $d \gg r_o$, the electric field induced in the plasma by the capacitor field E_o is then given by (Crawford *et al.*, 1963)

$$E = \frac{2E_o}{(2 - \frac{\omega_p^2}{\omega^2})}, \tag{93}$$

relating the resonance frequency to the plasma frequency, $\omega_r = \omega_p/\sqrt{2}$. It is thus *less* than the plasma frequency. Crawford *et al.* (1963) addressed in particular the modifications of Eq. (93) due to the presence of a static magnetic field, and Aničin (1965) considered the plasma-capacitor coupled oscillations in an LC circuit. Experimentally, higher order resonances also emerge, and Parker *et al.* (1964) have achieved good agreement between their measurements and a non-uniform hot-plasma model description. They also treated the quadrupole oscillations of a plasma column.

f) Power Feed. The geometry of the microwave power feed, and its location in the cavity or waveguide wall is decisive for the excited mode structure. The various feed schemes are essentially the same as with (a) waveguide-to-waveguide junctions, or (b) coaxial line-to-waveguide junctions (Ishii, 1966; Gandhi, 1981). A loop coupling (c.f. Fig. 6) induces locally a magnetic field perpendicular to the loop. Local electric field excitation can be achieved by a coaxial line, whose outer conductor is connected to the cavity wall, while its inner conductor protrudes slightly into the cavity. For waveguide-waveguide or waveguide-cavity junctions, iris couplings and slot couplings are used. The latter select a particular electric field polarization. The *location* of the power feed should match the location of the field maximum for the desired mode, for waveguides usually $\lambda/4$ away from

the end wall. For higher order modes, possibly several feeds at appropiate positions may be necessary.

g) Circuitry. The aim of the microwave circuitry is to detect the change in resonance frequency due to the susceptance change, $\mathrm{Re}(\epsilon)$, and/or the change in Q value due to the conductance change , $\mathrm{Im}(\epsilon)$. Both changes are caused by the presence of the plasma within the cavity (Harris and Balfour, 1965). A microwave discriminator (Pollard, 1980; Gandhi, 1981; Somlo and Hunter, 1985) provides the standard scheme for such standing-wave-ratio measurements that determine, respectively, the plasma density and the collision frequency. The discriminator consists of an oscillator (microwave generator), two hybrid tees, to which detectors and/or matched loads are attached, and a short-circuit plunger to balance the reflections from the cavity under off-resonance condition. A simplified, frequently used scheme retains one directional coupler (instead of the hybrid tee), and isolates the source by in-line attenuators (Biondi, 1951). Another method to directionally couple out the measured signal is the use of pick-up probes in the cavity, similar to the driving couplers discussed earlier (Schulz and Brown, 1955). The latter are a natural consequence when coaxial lines or TEM waveguides are used.

h) Source. A microwave source with some tunability, that depends on the envisioned density range, is required, be it manual or by sawtooth type frequency sweep. In the case that the plasma source is modulated or pulsed, the manual operation is simple but time consuming; the frequency swept operation requires a trigger in synch with the plasma source, possibly with an additional adjustable time delay provision (Biondi, 1951; Lieberman and Lichtenberg, 1969; Bisschops and de Hoog, 1985). The tuning range is limited by the frequency dependency of the discriminator components, particularly of the short-circuit plunger.

3. Microwave Reflectometry

Transmission and reflection measurements, c.f. Fig. 1, can be performed on plasmas that partially fill a waveguide, or by irradiating the plasma surface with microwave power (Vadnjal and Buffa, 1965). Transmission measurements are rare, since the density range

where this would be feasible is narrow. Either (a) the plasma is tenuous or optically thin at the used wavelength, and virtually all the microwave power is transmitted. Then the *dispersive* effects and to a lesser extent, the *refractive* effects are dominant. The dispersive effects are the basis for most cavity measurements, * and for interferometry. Exploiting the refractive effects for diagnostics would have to rely on complicated inverse ray tracing calculations and has, therefore, not been employed so far. Or (b) the plasma density is close or has reached the cutoff level, *and/or* it is much thicker than a penetration length. Then essentially all of the microwave power gets reflected, which is used for reflectometry (Anissimov *et al.*, 1960). This technique was used to characterize moving or stationary plasmas filling a waveguide segment (Bethke and Ruess, 1964; Minami and Takeda, 1969). Roughly speaking, the plasma acts as a waveguide termination, that can be determined by a bridge circuit or discriminator. If the plasma is not optically thick, but terminated by a shorting (wave reflecting) endplate that closes off the waveguide end, the same bridge technique can determine the *phase shift* after a double pass, and the *attenuation constant* the microwave has suffered by the plasma. This technique is a hybrid between a transmission measurement and interferometry, and requires that no appreciable power is reflected *off the plasma.* Bhattacharya, *et al.*, (1967) used this technique to monitor the ionizing radiation in a nuclear reactor. They also used the same bridge scheme for a radiometric determination of the electron temperature (see Sec. V).

IV. INTERFEROMETRIC TECHNIQUES

Microwave interferometry is one of the methods used to obtain the line integrated density of a plasma. This measurement, and the knowledge of the plasma dimensions give the average plasma density, one of the basic parameters needed to characterize a discharge. In contrast with probes (Chen, 1965), which can perturb the plasma to be measured, interferometry is non-intrusive.

A. Basic Relations

As a consequence of the dispersion properties of a plasma at microwave frequencies

* Even for $\omega_p > \omega$, the plasma still has to be optically thin to apply perturbation theory [c.f. Eq. (88)].

discussed in detail in Sec. II, a wave propagating through a plasma undergoes a phase shift relative to a wave propagating in vacuum. For a wave with an electric field parallel to the magnetic field in the plasma, the propagation properties are independent of the magnitude of the magnetic field. For this case, known as the ordinary mode, the wave number in the plasma is given by Eq. (56). In practice, for a waveguide carrying the fundamental TE_{10} mode, the electric field is parallel to the minor waveguide dimension.

In interferometry, the plasma whose density we would like to measure is inserted in one of the arms of a Mach-Zender interferometer, as shown for example in Fig. 7. The resulting phase shift between the waves traveling along paths of equal length, one through the plasma, and the other in the waveguide, is measured to determine the plasma line density. The phase shift $\Delta\phi$ is related to the plasma parameters by

$$\Delta\phi = \int_{-x_o}^{x_o} (k_o - k_x)dx = k_o \int_{-x_o}^{x_o} [1 - (1 - \frac{\omega_p^2}{\omega^2})^{1/2}]dx \tag{94}$$

where the integral is along the plasma path. The plasma frequency ω_p is given by Eq. (6). We have assumed that the collision frequency is much smaller than the microwave frequency and, therefore, the effects of collisional damping can be neglected. For $\omega_p^2 \ll \omega^2$ or, equivalently, for a plasma well below cutoff $n_e \ll n_c$, with n_c the critical density given by Eq. (11), the phase shift in units of 2π, i.e. the number of fringes, is given by

$$\begin{aligned} N = \frac{\Delta\phi(t)}{2\pi} &= 4.48 \times 10^{-18} \lambda_o \,(\text{cm}) \int n_e(x,t)dx \,(\text{m}^{-2}) \\ &= 1.34 \times 10^{-16} \frac{1}{f_o \,(\text{GHz})} \int n_e(x,t)dx \,(\text{m}^{-2}) \end{aligned} \tag{95}$$

where λ_o and f_o are the microwave vacuum wavelength and frequency, respectively.

B. Types of Interferometers

Although the basic interferometer configuration is common to all systems there is a great variety of methods to determine the phase shift. Next, we discuss some of the techniques typically used:

1. Bridge Interferometers

When the expected fringe shift $N \ll 1$, that is for low density plasmas, a bridge interferometer (Hotston and Seidl, 1965) is a simple system to set up. In this interferometer,

the microwave power from a source goes through a ferrite isolator and is then divided into two branches. One is used as a power monitor, the other goes through another directional coupler to obtain the two arms of the interferometer. Each leg contains a variable attenuator used to adjust the signal amplitudes in each leg. The reference leg contains in addition a phase shifter also used for the initial adjustments. A hybrid tee with two diode detectors after ferrite isolators is used as the detector assembly. A detailed discussion of the adjustments required is given by Hotston and Seidl. With a proper setup direct phase measurements are possible, since for small phase angles $\sin\Delta\phi \approx \Delta\phi$. Their system was limited to phase shifts $\Delta\phi \leq \pi/9$. One advantage is that the time response of the system is limited only by the detector response which can be several MHz (see also: Overzet and Verdeyen, 1986).

Another system (Lindberg and Eriksson, 1982) extended the phase evaluation to arbitrary phase angles by using exact analytical expressions of the detector response. A detailed discussion of the phase evaluation is discussed in their paper. In their system there is still an ambiguity at some values of the phase angle where it is not possible to determine whether the phase increases or decreases. They propose that an alternate density measurement such as probes could be used to eliminate this ambiguity. In cases where probes are impossible to use, phase quadrature techniques can be employed as discussed in Sec. IV.B.5.

2. Frequency Swept Interferometers

A schematic diagram for a serrodyne, frequency swept or "zebra" interferometer is shown in Fig. 7. The operation of the interferometer is as follows: an additional length of waveguide ΔL is introduced in one of the arms of the interferometer which produces a phase shift $\Delta\Phi = k_g \Delta L$, between the arms, where $k_g = 2\pi/\lambda_g$. The guide wavelength λ_g is frequency dependent and is given by

$$\lambda_g = \frac{1}{[(\frac{f_o}{c})^2 - (\frac{1}{2a})^2]^{1/2}} \tag{96}$$

where c is the speed of light and a the major dimension of rectangular waveguide.

The microwave source, either a klystron or Gunn oscillator, is swept in frequency

using a sawtooth of frequency f_{swp}. After an isolator, that prevents reflections back to the source, a side-arm coupler is used to split the power into the two interferometer arms. The detector is a double balanced mixer (Roddy, 1986), a device whose intermediate frequency (IF) output has two different frequency components given by the sum and difference of the input frequencies of the local oscillator (LO) and signal (RF) inputs. The sum frequency is naturally rejected by the frequency response of the circuitry used after the IF. In this interferometer, the plasma leg is connected to the RF input and the reference leg with the additional phase shift is connected to the LO, but the arrangement can be reversed. The microwave power in the LO leg should be high enough to drive the mixer. Its value depends on the unit and is typically 3 to 7 dBm.

The phase information from the plasma is contained in the difference frequency signal of the IF output, in which the microwave source frequency cancels. This term is proportional to $\cos(k_g(t)\Delta L - \Delta\phi(t))$. The time dependence of the argument is a consequence of the frequency sweep, i.e. k_g, and $\Delta\phi$, the phase shift produced by the plasma. For times less than a sawtooth period, the guide wave number is given by:

$$k_g(t) = k_g(0) + \frac{\Delta k_g}{2\pi}\Omega t = k_g(0) + \frac{1}{2\pi}\frac{dk_g}{df_o}\Delta f_o \Omega t \tag{97}$$

where Δf_o is the amount the source frequency is swept and $\Omega = 2\pi f_{\text{swp}}$.

Substituting for this value of k_g, the IF output has the form $\cos(n\Omega t - \Delta\phi + constant)$, where n is given by

$$n = \frac{1}{2\pi}\frac{dk_g}{df_o}\Delta f_o \Delta L = \frac{\Delta L}{\lambda_g}\left(\frac{\lambda_g}{\lambda_o}\right)^2 \frac{\Delta f_o}{f_o} \tag{98}$$

The interferometer is adjusted to obtain integer values of n, usually $n = 1$ or one complete cycle. In this case the IF output is modulated at the sweep frequency.

Since the oscillator has a limited frequency sweep range of typically several hundred MHz for Gunn oscillators, Eq. (98) is used to determine the required ΔL. In practice, ΔL is chosen taking into account the practical limitations in Δf_o and the amplitude of the sawtooth voltage is adjusted until a clean sine wave is obtained at the IF port. Usually, the output frequency of the source is not linear with the applied voltage over the entire range

of adjustment. When the required frequency sweep exceeds the linear range there will be some distortion of the sine wave at the IF port. If possible, ΔL should be chosen such that the amount of frequency sweep occurs over the linear range, however, this may require an excessively long waveguide and attenuation may become a problem. In addition, at the sawtooth resets there will be "fly-back" glitches in the signal. A tunable amplifier or a bandpass filter can eliminate the problems associated with the distortion and fly-back.

Finally, the IF output from the double balanced mixer is pre-amplified and sent to a phase detection system. The phase between a reference square wave from the sawtooth generator is compared to the square wave of the IF output that results from a bandpass filter and limiting amplifier. The phase sensitivity is $2\pi/16$ limited by the sweep frequency of 1 MHz and the response of the components used in the phase detection circuit. More details about phase detection techniques are given in Sec. IV.E.

3. Heterodyne Interferometers

As the plasma density and size increases, as in present day fusion experiments, the microwave frequency required to avoid cutoff and refraction problems, discussed in detail in Sec. IV.D.1, increases. It becomes necessary to use millimeter and submillimeter sources and techniques. At these higher frequencies, the available source power decreases rapidly, the losses in the transmission elements become significant and waveguide alignment needs to be accurate. It is therefore important to improve the sensitivity of the detection system. Heterodyne techniques, which involve the use of two different frequency sources, are quite powerful in this respect.

One example of such an interferometer (Cummins, 1970) operates as follows: a microwave source of frequency f_o is used as a local oscillator, a different source operating at frequency $f_o + f_m$ provides the plasma signal. Care has to be taken to keep the LO and main source locked to each other so that the difference frequency remains constant. This is accomplished using automatic frequency control (AFC) loops. The signals are combined in a mixer which provides an output at the intermediate frequency f_m which in turn contains the phase shift produced by the plasma. A local oscillator at frequency f_m is used

to detect this phase shift using phase quadrature techniques.

Some super-heterodyne receivers use several frequencies to eliminate frequency drifts in the transmitter and local oscillator (Efthimion *et al.*, 1985), using up and down conversion with appropiate filter stages. Other receivers (Coffield *et al.*, 1981, 1983) use two different intermediate frequencies (IF). A high radio frequency (several hundred MHz), is used to separate the microwave sources. The proper combination of mixers and local oscillators provides down conversion to another IF output which contains the plasma phase information. This second IF output, at a frequency of tens of MHz, is sent to phase comparator circuits to obtain the phase shift which is then stored in transient digitizers.

The complexity and cost of these systems increase tremendously in comparison with those previously described. The reader is referred to the references for more details on these techniques. Super-heterodyne receivers are widely used in scattering and radiometry which will be discussed in more detail in Sec. V.

4. Frequency Modulated Interferometers

A system developed by Ernst (1964), which operates on a similar principle as the heterodyne technique, uses a microwave source of frequency f_o which is split using a side arm coupler with one arm going to the LO input of a mixer. The other arm, goes through an isolator into a single side band modulator which generates an output with frequency $f_o + f_m$, where f_m is an intermediate frequency used in the modulation source. This wave traverses the plasma, undergoes a phase shift $\Delta\phi$ and goes to the RF input to the mixer. The mixer output of frequency f_m and which contains the plasma phase information is compared with a reference signal from the modulation source. Again, basic phase detection techniques can be used. The modulation frequency can be tens of MHz which allows excellent time resolution and the capability of using FM demodulation techniques (Jacobson, 1982) to obtain the phase. Phase digitizers are commercially available in this frequency range. One problem with this system is that single side band modulation at millimeter wavelengths has a conversion loss on the order of 30 dB. In addition, care should be taken in the suppression of the carrier or unwanted side bands generated in the modulator as discussed

in detail by Ernst.

A variant of the technique is given by Wallington and Beynon (1969). The standard microwave bridge, with a side arm coupler to split the power into the main and reference legs is used. However, two modulators are added in the plasma arm, one single side band modulator and a balanced modulator. Each is driven by frequency synthesized signals differing in frequency by 1 kHz, in their case, the single side band unit driven at 111.101 MHz and the balanced at 100.100 MHz. The reader is referred to their article for a detailed explanation of the different frequencies generated in these modulators. The net result is that the signal traversing the plasma differs by 1 kHz from the microwave source, and when both are combined in a mixer, a 1 kHz output results. The reference 1 kHz is obtained from mixing the two frequencies that drive the modulators. The phase difference is then determined with a counting circuit. High phase accuracy $2\pi/1000$ is obtained with a 1 MHz clock that drives the counting circuit.

5. Quadrature Interferometers

In these systems, signal outputs which are proportional to the sine and the cosine of the phase angle are generated simultaneously. Each signal can be digitized and a computer program used to calculate the phase as a function of time. The digitization rate should be high enough to prevent a phase change due to the plasma in excess of π between samples. If this is the case the program can evaluate the phase uniquely at each point and assume the smallest change in phase between adjacent time points in order to determine the direction in which the phase is changing.

In practice, such a system has been implemented by Kaiser *et al.* (1962). In their system the reference leg of the interferometer contains two mixer networks one of which is phase shifted by 90° with respect to the other. Brenning (1984) uses a similar method and describes in detail the initial setup required. A detailed analysis of the calculations needed to obtain the phase is presented in this reference.

An alternate method is used by Lister *et al.* (1982) in which a fast phase shifter (FPS) is used in the reference leg to provide a phase shift of 90° in a time much faster than

the time rate of change of the density. A single detector is used whose output signal is proportional to the sine of the phase during one time period, for example when the FPS is off, and then to the cosine during the next period when it is on. In practice, a four port circulator is used since at the frequency used (140 GHz) fast phase shifters are not available. The whole system is controlled by a microprocessor which also calculates the phase as a function of time. The time response of the system is limited by the number of computer cycles needed to evaluate the phase and the clock rate of the processor itself to 24 μsec. As in any quadrature method changes in phase should be less than π in each cycle which gives the upper limit in the line density changes measurable with this system.

6. Other Interferometers

When the time rate of change of the plasma is slow and the density is low, so that fringe shifts do not exceed 2π, commercially available lock-in amplifiers can be employed to obtain the phase (Levine *et al.*, 1965; Brown *et al.*, 1970).

A variant of the frequency swept systems (Sec. IV.B.1) can be used in which the waveguide path difference between the two legs can be substituted by a fast phase shifter (FPS) in one of the arms (Ernst, 1967). The microwave source is not swept in this case. After a directional coupler, the plasma or reference leg contains a y-junction circulator that routes the microwaves through the FPS, and a sawtooth is used to modulate the phase in the FPS. A double balanced mixer can be used as the detector. The IF output is identical to that previously described in Sec. IV.B.1. A similar system was used by Uckan (1984) to obtain a direct readout phase system. In his setup the voltage to the FPS is continuously adjusted using a feedback loop to keep the arms nulled. The output from the phase detector serves as the input to a current driver to the FPS. The voltage produced by this current across a resistor is therefore proportional to the phase change due to the plasma.

Another variant of the serrodyne system is obtained using a phase locked loop which changes the frequency of the microwave source (Strawitch *et al.*, 1986) such that the change due to the plasma is cancelled. In this case a measurement of the voltage at the source is

required to infer the phase. Some systems have used a Gunn oscillator simultaneously as source and detector (Bartlett and Brand, 1973).

C. Abel Inversion and Multi-Chord Interferometers

Interferometry provides only a line-integrated density measurement, therefore several radial chords need to be measured in order to obtain the density profile. Consider a cylindrical plasma of radius R which is azimuthally symmetric, and a phase measurement along a chord located at a distance h from the axis. The phase shift at each chord location is given by

$$\Delta\phi(h) = 2\int_h^R \frac{n_e(r)r\,dr}{\sqrt{r^2-h^2}}. \tag{99}$$

The inversion of this integral equation for $n_e(r)$, known as the Abel inversion formula is:

$$n_e(r) = -\frac{1}{\pi}\int_r^R \frac{d\Delta\phi}{dh}\frac{dh}{\sqrt{h^2-r^2}}. \tag{100}$$

Even in the case of azimuthal symmetry considered here, it becomes immediately apparent that since the value of the derivative of the phase shift is required, a large number of chord measurements is needed to infer the density. In practice, it is useless to increase the number of channels too much since the accuracy of the measurement is limited by the accuracy in $\Delta\phi$, which is typically 5 to 10 %. In addition, the complexity of the system and its cost increase usually limit the number of channels to the range of 5 to 10. When the number of available channels is small (< 5), there is often not enough information to infer the profile using Abel inversion. For these cases the line density is calculated using assumed density profiles (Demas *et al.*, 1985) with several fitting parameters. Alternatively, a constant density, trapezoidal, parabolic or Gaussian density profiles can be used to calculate the line density. These profiles involve only a few parameters which can be determined using least squares fitting techniques. In this manner, the profile and plasma parameters which best fit the experimental data can be obtained. Another useful technique involves the use of a derivative free inversion formula (Deutsch and Beniaminy, 1982) which can decrease the errors incurred in the differentiation of experimental data. When the assumptions of azimuthal symmetry cannot be made it becomes necessary to use more than one view of the plasma (Sauthoff and von Goeler, 1979; Wetzer, 1983). This is the same technique

used in tomographic reconstruction for which inversion algorithms are readily available (Huesman *et al.*, 1977).

Experimentally, in cases where the plasma is in steady state or it is highly reproducible, a movable single channel system can be sufficient (Uckan, 1983). In this system, a horn-lens (Uckan, 1981) arrangement with 45° mirrors is used to eliminate attenuation problems caused by material wall flaking. In transient discharges however, multi-chord systems are often required to obtain density profiles for each discharge. Such information is needed to understand the plasma properties and transport in each experiment. In a frequency swept multi-chord system using a single source (Lisitano, 1975), there can be crosstalk between adjacent channels. In this case, it is possible to use different values of ΔL for each chord. With this method, several harmonics of the sawtooth frequency are obtained and a tunable amplifier for each channel is used to eliminate crosstalk. Waveguide attenuation as ΔL increases may become important, especially at higher microwave frequencies. In these cases it becomes necessary to use overmoded waveguide to reduce the power losses. When several channels are fed from a single microwave source, there should be enough power available for each channel. Alternatively, each channel can be fed using individual sources (Sevillano *et al.*, 1984). The power requirements depend on the detection method and the components chosen, which we discuss in more detail in Sec. IV.D.2.

A horn-lens arrangement is used by Casper *et al.* (1986) to generate a microwave beam that scans the plasma. In this system, two perpendicular views are used to obtain tomographic reconstruction information. An array of closely spaced horns is used as receivers in this system.

D. Interferometer Design

A practical and simple approach to interferometer design is given which should be useful to the novice in microwave interferometry and techniques. A basic knowledge or expectation of the plasma density and dimensions is required at the outset. There is also a need to specify the requirements we would like to be met by our system which vary in each application. These may include the time response needed, accuracy of the measurements,

stability of the system with respect to long time drifts, etc. The issues that need to be considered when designing an interferometric system can be divided into:

(a) Physics issues related to the properties of the plasma under investigation, such as wave propagation properties, plasma size and its relation to probing wavelength, refraction effects, cutoff and plasma lifetime.

(b) Practical issues such as phase sensitivity, unambiguous density tracking, microwave source power, electrical noise immunity, maintenance, ease of operation, cost, convenient data acquisition and display.

(c) Specific issues that may be unique to the application, such as vacuum needs, elimination of reflections, access to the plasma chamber, etc. The large variety of such specific requirements exceeds the scope of this chapter and must be addressed on a case-by-case basis. Therefore, meeting them is left to the ingenuity of the experimentalist.

1. Choice of Microwave Frequency

This is the most basic yet most important step in the design. The microwave frequency required is determined by the physical properties of the plasma under investigation. In addition, its value has important implications on a variety of other issues such as phase sensitivity, system cost, availability of power sources, etc. We first consider the physics of the microwave propagation and then some of the practical issues.

From the physics standpoint, we need to consider: a) plasma size, b) cutoff and c) refraction.

a) Plasma Size. The basic assumptions made in Sec. II.E.1 used in the derivation of Eq. (56) need to be satisfied. These require a plasma size large compared to the wavelength of the probing beam. From a practical point of view, the spatial resolution of the system is limited by the fact that it is not possible to focus a microwave beam to a size smaller than a few wavelengths (Sec. II.F). In addition, the wavelength in the plasma increases due to its dispersion properties. Typically, it is required that the characteristic transverse plasma size d must satisfy $d > 5\lambda_o$ (Ernst, 1972).

b) Cutoff. If the plasma density increases such that $\omega_p^2 > \omega^2$, or $n_e > n_c$ the critical

density given in Eq. (11), the microwave beam does not propagate through the plasma; it is cut off. Although a measurement of the transmitted power can be used to determine when the microwave beam is cut off, and thus the density at that time, this technique only provides a lower bound on the density. In interferometry, it is useful to determine the density unambiguously at all times during the discharge. Therefore the frequency chosen must be high enough to avoid cutoff. It is usually enough to choose $n_c > 3n_e$. Note that near cutoff Eq. (95) needs to be replaced by the exact form Eq. (94).

c) Refraction. Refractive effects usually pose a more stringent condition on the microwave frequency than cutoff. It is of particular importance for the design of multi-chord systems where refraction near the edge may deflect the beam out of the receiver. In the presence of density gradients a microwave beam is refracted according to Snell's law (Born and Wolf, 1980). The total angle of refraction can be calculated by integration over the path length. It is given by (Shmoys, 1961)

$$\alpha = \int_{-x_o}^{x_o} \frac{\nabla n}{n} dx \tag{101}$$

To estimate the refraction angle some assumptions about the plasma density profile must be made. A parabolic density profile given by $n_e = n_o(1 - r^2/r_p^2)$ where n_o is the density on axis and r_p the plasma radius can be solved analytically. In this case, the maximum refraction angle calculated from Eq. (101) is given by $\alpha_{\max} = \sin^{-1} \frac{n_o}{n_c}$. This maximum refraction occurs near the edge. Although because of symmetry, α vanishes for the chord on axis, refraction effects should be considered even when designing a single channel on axis. Under some conditions, due for example to the presence of instabilities, density gradients can move across the beam causing refraction.

When designing a multi-chord system the maximum angle is limited by deviations from a chord measurement and the possibility of crosstalk between adjacent channels. The maximum refraction angle may therefore be limited by the total number of channels in the system M. The maximum refraction angle is in this case inversely proportional to M. In systems with high gain horns, commonly used to provide beam directivity and because of power transmission requirements, the refraction angle α should be smaller than the

acceptance angle of the horn, otherwise no power will be coupled. The acceptance angle of a horn depends on its gain (Gandhi, 1981; Bhartia and Bahl, 1984).

It is useful to consider a practical example of a plasma with peak density $4 \times 10^{18}\,\mathrm{m}^{-3}$, using 25 dB gain optimum horns. Usually the plasma is uniform along one direction (otherwise we would also need to measure the density profile in that direction). Therefore, either the H-plane refraction angle or the E-plane needs to be considered. For a cylindrical plasma with a magnetic field along the axis of the cylinder, H-plane refraction is the important one. For an optimal horn of gain G, the half-power beam width is given by $\alpha_h = 80°/\sqrt{G/(2\pi 0.81)}$ (Ghandi, 1981), which translates to a condition on the critical density of $n_c > 5.9 n_o$. This is a factor of 2 larger than the required cutoff condition. The microwave frequency is then $f_o > 44$ GHz.

Next we consider some of the practical issues. As in most designs, there are conflicting requirements. Whereas cutoff and refraction indicate the use of higher microwave frequencies, phase sensitivity decreases with frequency as in Eq. (95). Thus selecting a frequency that is too high may limit the dynamic range of the interferometer. System cost is almost always an important consideration, and as the microwave frequency increases microwave components cost increases rapidly. In addition, power sources and levels are more scarce. If possible, it may be better to select frequencies commonly used commercially, such as for example 10 GHz or 24 GHz, for which many inexpensive components are readily available.

2. Choice of Interferometer Type

Aside from the practical issues such as cost, maintenance, ease of operation, etc., there are also important physical limitations to consider such as phase sensitivity and time resolution. Of the latter, time resolution may be the most important consideration when choosing a particular interferometer system.

Bridge interferometers are comparatively inexpensive but require careful initial setup and adjustments (Hotston and Seidl, 1965). Unless used for low densities, where the fringe shifts are small $N \ll 1$, the evaluation of the phase angle can be ambiguous (Lindberg and Eriksson, 1982). Their main advantage is a good frequency response, several MHz, limited

by the detectors used.

The time response of serrodyne systems is limited to the sweep rate of the source frequency and the availability of digital techniques to evaluate the phase shift. As previously mentioned a 1-MHz system is easily accomplished using commercially available phase digitizers with a fringe resolution of $2\pi/16$. Better fringe resolution can be obtained at lower sweep frequencies.

Frequency modulated systems can have good frequency response, on the order of the modulation frequency. One advantage of these systems is that quadrature phase detection techniques are easy to implement using off-the-shelf components. Commercial phase digitizers are also available. An important disadvantage is the low conversion efficiency of the side band modulators in the millimeter range. Heterodyne systems have similar time response and advantages albeit they can be complicated. Their sensitivity makes them the natural choice when power levels are not high, usually at high microwave frequencies.

3. Power Requirements

The minimum power that is acceptable at the detector depends among other things on the experimental noise environment, the type of interferometer chosen and the detector sensitivity. It is not possible to give a number that applies to all situations. The value of the signal-to-noise ratio at the detector should be decided upon and working back through the microwave network the losses caused by the components, waveguide transmission, plasma and vacuum propagation losses, etc. are calculated to obtain the desired output power at the source. We discuss some examples.

a) Component Losses. It is important to consider insertion losses, which gives a measure of the power loss in transmission through a device or network. Single side band modulators mentioned earlier have a large insertion loss, on the order of 30 dB. Reflection losses caused by impedance mismatch between components can be calculated using the voltage standing wave ratio (VSWR) of the device. In this case the voltage reflection coefficient ρ_v is given by

$$\rho_v = \frac{\text{VSWR} - 1}{\text{VSWR} + 1}. \tag{102}$$

Since power goes as the square of the voltage the reflected power is given by ρ_v^2.

b) Transmission Losses. We consider waveguide and vacuum losses. As the microwave frequency increases, dissipation caused by the finite resistivity of the waveguide material becomes important. The theoretical attenuation can be calculated in terms of this resistivity, waveguide dimensions and microwave wavelength. Attenuation in rectangular waveguide is discussed in detail by Benson (1969). When using the theoretical formula, it is important to know that the discrepancy between the calculated and measured value increases with frequency, particularly in the case of copper guides. Measured values of the attenuation for copper guides at 35 GHz and 70 GHz are respectively 0.65 dB m^{-1} and in the range 3.5-5.3 dB m^{-1}. Etching of the waveguide followed by hydrogen annealing gives closer agreement with the theoretical values. This shows the importance of waveguide etching and cleaning techniques required when waveguide sections are built rather than purchased. The number of flanges, elbows, twists, etc. should be minimized to avoid losses at each connection. Waveguide benders can be fabricated to allow more complicated waveguide paths with a minimum of breaks in the guide.

The attenuation values given above indicate that waveguide losses in the fundamental mode become unacceptable at high microwave frequencies. A simple solution for low-loss transmission over moderate distances up to about 30 m is the use of an overmoded guide (Robson, 1969). Commercially available tapered transitions are used to connect the fundamental to the larger, overmoded waveguide. Important considerations when using overmoded guides are losses, mode conversion in bends, tapers and other discontinuities and trapped-mode resonances. Experimental data on losses in overmoded guides are not as extensive as for fundamental guides (Robson, 1969). To avoid mode conversion in bends, gradual bending is required, with radius of curvature greater than 20 times the wavelength. Trapped-mode resonances (Robson, 1969; Bhartia and Bahl, 1984) in configurations when there are transitions to fundamental guide at each end of the transmission line, can reduce substantially the transmitted power due the excitation of standing cavity modes in the larger guide.

Power attenuation caused by the plasma, which can become serious near cutoff, needs to be estimated. In addition, there will be losses in the transmission through the vacuum. To obtain plane waves incident upon the plasma, a condition that was assumed in the derivation of Eq. (56), the distance d from the horn to the plasma should satisfy $d \gtrsim 2D^2/\lambda_o$, where D is the largest horn dimension. In this case, the received power P_r at the antenna is related to the transmitted power P_t by

$$P_r = \frac{\lambda_o^2 G_t G_r}{16\pi^2 R^2} P_t \tag{103}$$

where G_t and G_r the gains of the horns, and R their separation. The gains are usually given in reference to an isotropic radiator. Open ended waveguides are sometimes used instead of horns (Efthimion *et al.*, 1985). As for horns, the open ended gain can also be computed (Gandhi, 1981).

4. Choice of Components

It is outside the scope of this chapter to discuss in detail the great variety of microwave components available. Microwave technology books which have kept up-to-date (Heald and Wharton, 1978; Gandhi, 1981; Bhartia and Bahl, 1984; Roddy, 1986) are instead a valuable source which can help in the understanding of the operation of microwave devices. Examples of possible applications are also given in such references. We will restrict our discussion to a few examples.

Ferrite isolators are frequently used in interferometer systems to eliminate reflections back to the source or in detector assemblies. When working in regions of high magnetic field, often found in fusion experiments, it is necessary to provide magnetic shielding to such devices. A high permeability material, soft iron for example, surrounding the device is commonly used. The material should be thick enough to be below magnetic saturation (Jackson, 1975).

Power dividers frequently used include side-arm couplers and hybrid tees. Tees are also employed in detector assemblies.

Attenuators and phase shifters are needed in some of the bridge and quadrature tech-

niques discussed above in order to balance each of the interferometer arms. Usually, they are of limited use in serrodyne systems. Phase shifters can simulate the presence of the plasma and therefore can be used to check and calibrate the system.

When selecting horns, size may be an important consideration because of restricted access to the plasma chamber. In those cases where a particular design is needed, the properties of horn antennas can be found in the literature (Love, 1976; Heald and Wharton, 1978; Gandhi, 1981; Bhartia and Bahl, 1984; Roddy, 1986). Microwave component manufacturers can usually fabricate them to order although this may be expensive. Generally, standard gain horns are adequate. They have the advantage that they are commercially available and their gain and emission patterns are readily available from the manufacturer. If length is a problem, the commercial horns can be easily cut, which would be cheaper than ordering a special unit. The gain of the shortened horn should be calculated or measured.

Mixers are an important component in most systems. There are several kinds (Roddy, 1986) depending on the number of diodes used in the mixing process. Single diode mixers can be used when the signal levels are relatively high and noise is not a problem. Balanced mixers use two diodes and provide no isolation between the RF and IF ports. Double balanced mixers provide isolation between all the ports and are the preferred choice when signal levels are small. Isolation between the ports, especially between LO and RF, and LO and IF is an important parameter when specifying a mixer. We recall that the LO power is typically much higher than the RF power ($\sim$ 7 dBm), the higher this ratio the better is the isolation. The noise figure, the required signal-to-noise ratio and the isolation are used to determine the lowest acceptable input signal.

E. Phase Detection Techniques

Digital, quadrature and FM demodulation techniques can be used to obtain the values of the phase. In digital techniques, the phase is obtained using comparator circuits or counters. For frequency swept interferometers, with $f_{swp} < 1$ MHz, a system developed at the Princeton Plasma Physics Laboratory (Greenberger, 1978) can be used. Detailed

schematics and an explanation of the operation are given in that reference. Briefly, with a master clock at 16 MHz, limited by the frequency response of the components used, the phase sensitivity is $2\pi/16$ at 1 MHz. Improved fringe resolution is obtained at lower sweep frequencies. Using this technique a phase digitizer for CAMAC is commercially available.

In frequency modulated or heterodyne interferometers the phase information is contained in a higher frequency carrier, typically tens of MHz. A phase comparator circuit using fast ECL logic has been developed (Coffield *et al.*, 1981). The phase comparison is made by a pair of flip-flops, one for the LO reference and the other for the signal, clocked to give an output pulse whose duration is given by the time difference between the input signals. The outputs from the flip-flops are low-pass filtered and go to a differential amplifier which gives an output voltage proportional to the phase shift. The phase range, given by the number of total fringes, is adjustable.

At tens of MHz, quadrature phase detectors can also be used. In these, the sine and cosine of the phase angle are generated and stored in digitizers. The phase is then computed from the arctangent. The digitization rate should be large enough to avoid phase changes greater than π between time samples. If this is the case the phase can be determined assuming the smallest phase change between samples. Phase detectors are commercially available but they can also be built using discrete components. A schematic diagram for a quadrature phase detector is given in Fig. 8. In this circuit, the phase difference at the mixer inputs should be carefully adjusted to 90°. At these frequencies, proper grounding techniques are required when building these circuits.

An output proportional to the phase can also be obtained using FM demodulation techniques (Jacobson, 1982).

V. MICROWAVE SCATTERING AND RADIOMETRY

The measurement of the scattering of electromagnetic radiation by the electrons in a plasma is a powerful diagnostic used in the determination of the electron temperature and density, ion temperature and electron density fluctuation spectra. In addition, the emission of radiation at the electron cyclotron frequency is used in fusion devices in the

determination of the electron temperature. This is particularly useful in Tokamaks where the magnetic field depends on the major radius of the device thus providing a radial profile measurement of the electron temperature.

To cover in detail the theory of scattering of electromagnetic waves or the emission of radiation in plasmas is outside the scope of this chapter. For details on scattering the reader is referred to Evans and Katzenstein (1969) or Sheffield (1975). A simple treatment is also given in Tsukishima (1979) and a review by Cano (1979). Radiation from plasmas is covered in Bekefi (1966). A recent review of cyclotron radiation measurements is given in Bornatici *et al.* (1983). A review of the instrumentation used in both techniques is given by Luhmann and Peebles, (1984).

A. Microwave Scattering

Electrons accelerated by the electric field of the incident wave re-radiate such that the resulting scattered signal satisfies energy and momentum conservation given by

$$\omega_s = \omega_o \pm \omega \quad \text{and} \quad \vec{\mathbf{k}}_s = \vec{\mathbf{k}}_o \pm \vec{\mathbf{k}}, \tag{104}$$

where $(\omega_s, \vec{\mathbf{k}}_s)$ are the angular frequency and wave vector of the scattered wave, $(\omega_o, \vec{\mathbf{k}}_o)$ those of the incident monochromatic wave and $(\omega, \vec{\mathbf{k}})$ characterize the fluctuations being studied. The amplitude of the wave number for the fluctuations is obtained from trigonometric relations for the triangle formed by the three wave vectors $\vec{\mathbf{k}}$, $\vec{\mathbf{k}}_s$ and $\vec{\mathbf{k}}_o$ which satisfy (104). It is assumed that the amplitude of the scattered wave vector is the same as the incident, which implies the momentum tranfer to the electron is negligible. The resulting relation is known as the Bragg condition

$$k = 2k_o \sin(\theta/2) \tag{105}$$

where θ is the scattering angle chosen.

The scattering parameter α determines the scattering regime under investigation. It is defined as

$$\alpha = \frac{1}{k\lambda_D} = \frac{\lambda_o}{4\pi\lambda_D \sin(\theta/2)}, \tag{106}$$

where $\lambda_D = (\epsilon_o kT/n_e e^2)^{1/2}$ is the Debye length. There are two regimes of α to consider: (a) $\alpha \ll 1$ which applies for the density range in present day fusion experiments for incident wavelengths in the visible or near infrared unless $\theta \sim 0$. For this case the scattering comes from individual unscreened electrons and the spectrum determines the electron temperature. (b) $\alpha \geq 1$, in this regime scattering can be used to determine the ion temperature or the level of fluctuations in the plasma. For wavelengths in the microwave region this condition is satisfied for nearly all of the scattering angles θ chosen.

The scattering cross section in a plasma can be calculated from classical electrodynamics. The resulting cross section is proportional to the quantity $S(\vec{\mathbf{k}},\omega)$, the dynamic form factor, defined as

$$S(\vec{\mathbf{k}},\omega) = \frac{1}{2\pi n_e V_s} \int_{-\infty}^{\infty} d\tau e^{i(\omega_s - \omega_o)\tau} \overline{n(\vec{\mathbf{k}},t) n^*(\vec{\mathbf{k}},t+\tau)}, \tag{107}$$

where n_e is the electron density, V_s the scattering volume, $n(\vec{\mathbf{k}},t)$ is the Fourier transform of the electron density, the asterisk denotes the complex conjugate and the bar implies a time average.

The differential scattered power per unit solid angle $d\Omega$ and angular frequency can be written in terms of the form factor as follows

$$\frac{d^2 P_s}{d\omega d\Omega} = n_e V_s p_o \sigma_T S(\vec{\mathbf{k}},\omega), \tag{108}$$

where $p_o = (1/2)c\epsilon_o E_o^2$ is the power density of the incident radiation, $\sigma_T = (e^2/mc^2)^2(1 - \sin^2\theta\cos^2\phi_o)$ is the Thomson cross section for scattering of electromagnetic radiation by electrons, ϕ_o is the angle between the electric field vector of the radiation and the plane of observation (usually one chooses $\cos\phi_o = 1$) (Sheffield, 1975).

In terms of the density fluctuations the total scattered power is given by

$$P_s = p_o \sigma_T V_s^2 \overline{|n|_{\vec{\mathbf{k}}}(t)^2} \Delta\Omega_r, \tag{109}$$

where $\Delta\Omega_r$ is the angle subtended by the receiver. An absolute calibration of the scattered power is usually performed using sources at known temperatures. The value of the

fluctuations can thus be obtained. Because the Thomson cross section is so small and the microwave power available is not large (less than 1 kW), it is necessary that the fluctuations are not of thermal origin but instead caused by instabilities or collective plasma motion to be observable.

1. Measurement Techniques

Some of the techniques already mentioned in interferometry are directly applicable to scattering. The frequency used for the scattering must be high enough so that refraction is not significant. In addition, the scattering parameter $\alpha \gg 1$ to measure collective fluctuations and the frequency response of the detector must be in the range of the expected instability. A spectrum analyzer is commonly used to obtain all the frequency information. Basically there are two methods of detection: Homodyne and heterodyne. Homodyne systems are simpler and involve only one microwave source, examples are given in the literature (Okabayashi and Arunasalam, 1977; Paris and Hollenstein, 1983; Rohatgi *et al.*, 1985). In heterodyne systems (Doane, 1980; Machuzak *et al.*, 1986) more than one microwave source is used, leading to more complexity. The sensitivity of these systems is greatly improved over homodyne and when measuring fluctuations which also involve plasma rotation they allow the determination of the direction of rotation.

At each scattering angle only a particular value of $\vec{k}$ is obtained. In many cases it is necessary to measure the scattering at several scattering angles to properly identify the mode present in the plasma (Goldston *et al.*, 1976; Paris and Hollenstein, 1983)

B. Radiometry

The measurement of the radiation from a plasma can be used to obtain information about the electron temperature. For a Maxwellian plasma the radiation intensity is given by

$$I(\omega) = \frac{\omega^2 k T_e}{8\pi^3 c^2} \frac{(1 - e^{-\tau})}{(1 - \zeta e^{-\tau})}, \tag{110}$$

where τ is the optical depth, and ζ the chamber reflectivity which depends on the optical system. Frequently, the frequency is chosen so that the plasma behaves as an optically thick ($\tau \rightarrow \infty$) object to the radiation. The temperature of the emitter can then be

determined. The temperature can also be determined using the ratio of the emission intensity from successive harmonics (Celata and Boyd, 1977). The density can also be obtained from optically thin harmonics if the temperature is known (e.g. from an optically thick harmonic).

2. Measurement Techniques

Conventional millimeter heterodyne receivers are the most commonly used (Taylor *et al.*, 1985 and 1986). When broadband detectors like InSb are employed a frequency analyzing element is also needed. Examples are Fourier-transform spectrometers (Costley *et al.*, 1974; Bartlett *et al.*, 1978), Fabry-Perot interferometers (Walker *et al.*, 1981) or grating spectrometers (Rutgers and Boyd, 1977).

REFERENCES

Adler, R.B. (1960), Chu, L.J. and Fano, R. "Electromagnetic Energy, Transmission and Radiation", Wiley, New York.

Agdur, B., and Enander, B. (1962), *J. Appl. Phys.* **33**, 575.

Akulina, D.K. (1965), "Proceedings VIIth International Conference on Phenomena in Ionized Gases", Beograd, Vol. 3, p. 74.

Aničin, B.A. (1965), *op. cit.*, p. 143.

Anissimov, A.I. (1960), Vinogradov, N.I., Golant, V.E., and Konstantinov, B.P., *Zhurn. Tekhn. Fiz.* **30**, 1009.

Anissimov, A.I. (1965), Budnikov, V.N., Vinogradov, N.I., and Golant, V.E., "Proceedings VIIth International Conference on Phenomena in Ionized Gases", Beograd, Vol. 3, p. 86.

Armand, N.A. (1982), Lisitskaya, A.A., Rogashkov, S.A., Rogashkova, A.I., Chmil', A.I., and Shustin, E.G., *Sov. J. Plasma Phys.* **8**, 212.

Asmussen, J., Jr. (1974), Mallavarpu, Raghuveer, Hamman, J.R., and Park, Hee Chung, in "Proceedings of the I.E.E.E.", **62**, 109.

Bartlett, D.V., and Brand, G.F. (1973), *J. Phys. E:* **6**, 1213.

Bartlett, D.V. (1978), Costley, A.E., and Robinson, L.C., *Infrared Phys.* **18**, 749.

Bekefi, G. (1966), in "Radiation Processes in Plasmas", John Wiley and Sons, New York.

Benson, F.P. (1969), Attenuation of Rectangular Waveguides, in "Millimeter and Submillimeter Waves", (F.P. Benson ed.), Iliffe Books Ltd., London.

Bethke, G.W., and Ruess, A.D. (1964), *Phys. Fluids* **7**, 1446.

Bhartia, P., and Bahl, I.J. (1984), "Millimeter Wave Engineering and Applications", Wiley, New York.

Bhattacharya, A.K. (1967), Verdeyen, J.T., Adler, F.T., and Goldstein, L. *J. Appl. Phys.* **38**, 527.

Biondi, M.A. (1951), *Rev. Sci. Instr.* **22**, 500.

Biondi, M.A., and Brown, S.C. (1949), *Phys. Rev.* **75**, 1700.

Bisschops, T.J., and de Hoog, F.J. (1985), *Pure Appl. Chem.* **57**, 1311.

Bize, D. (1965), Cadart, M., and Consoli, T., in "Proceedings VIIth International Conference on Phenomena in Ionized Gases", Beograd, Vol. 3, p. 74.

Born, M., and Wolf, E. (1980), "Principles of Optics", 6th ed., Pergamon.

Bornatici, M. (1983), Cano, R., De Barbieri, O., Engelmann, F., *Nucl. Fusion* **23**, 1153.

Brenning, N. (1984), *J. Phys. E:* **17**, 1018.

Brown, J. (1953), "Microwave Lenses", Wiley, New York.

Brown, Ian G. (1970), Compher, Alan B., and Hopkins, Donald B., *Rev. Sci. Instr.* **41**, 600.

Buchsbaum, S.J. (1960), Mower, Lyman, and Brown, S.C., *Phys. Fluids* **3**, 806.

Cano, R., (1979), in "Diagnostics for Fusion Experiments", (E. Sindoni and C. Wharton, eds.), Pergamon Press.

Casper, T. (1986), Stever, R., Rice, B., and Zammit, R., *Bull. Am. Phys. Soc.* **31**, 1619.

Celata, C.M., and Boyd, D.A. (1977), *Nucl. Fusion* **17**, 735.

Chapman, B. (1980), "Glow Discharge Processes", Wiley, New York.

Chen, Francis F. (1965), "Electric Probes", in "Plasma Diagnostic Techniques", (R.H. Huddlestone and S.L. Leonard eds.), Academic Press, New York.

Chen, F.F. (1984), "Plasma Physics and Controlled Fusion", Vol. 1, 2nd ed., Plenum, New

York.

Chen, F.F. (1968), Etievant, C., and Mosher, D., *Phys. Fluids* **11**, 811.

Coffield, F.E. (1981), Stever, R.D., and Lund, N.P., in "Proceedings of the 9th Symposium on Engineering Problems of Fusion Research", Chicago. Vol. 1, p. 961.

Coffield, F.E. (1983), Thomas, S.R., Lang, D.D., and Stever, R.D., in "Proceedings of the 10th Symposium on Fusion Engineering", Philadelphia. Vol. 2, p. 1920.

Cornbleet, S. (1976), "Microwave Optics", in "Pure and Applied Physics", Vol. 41, (H.S.W. Massey and K.A. Brueckner, eds.), Academic Press.

Cornbleet, S. (1984), "Microwave and Optical Ray Geometry", Wiley, New York.

Costley, A.E. (1974), Hastie, R.J., Paul, J.W.M., and Chamberlain, J., *Phys. Rev. Lett.* **33**, 748.

Crawford, F.W. (1963), Kino, G.S., and Cannara, A.B., *J. Appl. Phys.* **34**, 3168.

Cummins, W.F. (1970), *Rev. Sci. Instr.* **41**, 234.

Dattner, A. (1961), in "Proceedings Vth International Conference on Ionization Phenomena in Gases", Munich, Vol. 2, p. 1477.

Davis, L.W., and Patsakos, G. (1983), in "Proceedings of SPIE- the International Society for Optical Engineering", Vol. 423: Millimeter Wave Technology II, (J.C. Wiltse, ed.), p. 40.

Demas, N.G. (1985), Ma, C.H., Hutchinson, D.P., and Staats, P.A., *I.E.E.E. Trans. Plasma Sci.* **PS-13**, 41.

Deutsch, Moshe and Beniaminy, Israel (1982), *Appl. Phys. Lett.* **41**, 27.

Doane, J.L. (1980), *Rev. Sci. Instr.* **51**, 317.

Efthimion, P.C. (1985), Taylor, G., Ernst, W., Goldman, M., McCarthy, M., Anderson,

H., and Luhmann, N.C., *Rev. Sci. Instr.* **56**, 908.

Ernst, William P. (1964), *I.S.A. Trans.* **3**, 9.

Ernst, W.P. (1967), Princeton Plasma Physics Laboratory Report MATT-535.

Ernst, W.P. (1972), *I.E.E.E. Trans. Nucl. Sci.* NS-19, 740.

Evans, D.E., and Katzenstein, J. (1969), Rep. Prog. Phys. **32**, 207.

Fano, R.M. (1960), Chu, L.J., and Adler, R.B., in "Electromagnetic Fields, Energy and Forces", Wiley, New York.

Faugeras, P.E. (1965), in "Proceedings VIIth International Conference on Phenomena in Ionized Gases", Beograd, Vol. 3, p. 119.

Fellers, R.G. (1962), *The Microwave J.* **5**, 80.

Fessenden, T.J., and Smullin, L.D. (1965), in "Proceedings VIIth International Conference on Phenomena in Ionized Gases", Beograd, Vol. 3, p. 83.

Gandhi, Om P. (1981), "Microwave Engineering and Applications", Pergamon.

Golant, V.E. (1960), *Zhurn. Tekhn. Fiz.* **30**, 1265.

Golant, V.E. (1984), "Methods of Diagnostics Based on the Interaction of Electromagnetic Radiation with a Plasma", in "Handbook of Plasma Physics", (M.N. Rosenbluth and R.Z. Sagdeev, eds.), Vol. 2, Elsevier.

Goldston, R.J. (1976), Mazzucato, E., Slusher, R.E., and Surko, C.M., in "Proceedings of the VIth International Conference on Plasma Physics and Controlled Nuclear Fusion Research", Berchtesgaden, IAEA Vienna. Vol. I, p. 371.

Greenberger, A. (1978), Princeton Plasma Physics Laboratory Report PPPL-1466.

Harris, J.H., and Balfour, D. (1965), in "Proceedings VIIth International Conference on Phenomena in Ionized Gases", Beograd, Vol. 3, p. 79.

Heald, M.A., and Wharton, B.C. (1978), "Plasma Diagnostics with Microwaves", Robert E. Krieger Publishing Company, New York.

Herlin, M.A., and Brown, S.C. (1948), *Phys. Rev.* **74**, 291.

Hermansdorfer, H. (1968), "Microwave Diagnostic Techniques", in "Plasma Diagnostics", (W. Lochte-Holtgreven ed.), North-Holland, Amsterdam, p. 478.

Hotston, E., and Seidl, M. (1965), *Rev. Sci. Instr.* **42**, 225.

Huesman, R.H. (1977), Gullberg, G.T., Greenberg, W.L., Budinger, T.F., "Donner Algorithms for Reconstruction Tomography", Lawrence Berkeley Lab. Publication 214.

Ishii, T.K. (1966), "Microwave Engineering", The Ronald Press, New York.

Jackson, J.D. (1975), "Classical Electrodynamics", 2nd ed., Wiley, New York.

Jacobson, A.R. (1982), *Rev. Sci. Instr.* **53**, 918.

Jones, A.R., and Wooding, E.R. (1965), in "Proceedings VIIth International Conference on Phenomena in Ionized Gases", Beograd, Vol. 3, p. 122.

Kaiser, J.A. (1962), Smith, H., Pepper, W., and Little, J., *I.R.E. Trans. MTT***10**, 548.

Kato, K., and Hutchinson, I.H. (1984), M.I.T. Plasma Fusion Center Report PFC/RR-84-11.

Künstler, F. (1965), in "Proceedings VIIth International Conference on Phenomena in Ionized Gases", Beograd, Vol. 3, p. 93.

Levine, A. (1965), Kuckes, A., and Skislak, A., Princeton Plasma Physics Laboratory Report MATT-369.

Lieberman, M.A., and Lichtenberg, A.J. (1969), *Phys. Fluids* **12**, 2109.

Lindberg, L. and Eriksson, A. (1982), *J. Phys. E:* **15**, 548.

Lisitano, G. (1975), "Density Distribution Measurements in Large CTR Devices", in "Course on Plasma Diagnostics and Data Acquisition Systems" (A. Eubank and E. Sindoni, eds.), CNR Euratom, Varenna.

Lisitskaya, A.A., and Shustin, E.G. (1981), *Instrum. Exp. Tech. (USSR)* **24**, 158.

Lister, J.B. (1982), Means, R.W., and Oberson, P., *Rev. Sci. Instr.* **53**, 600.

Love, A.W. (1976), (ed.) "Electromagnetic Horn Antennas", I.E.E.E. Press Selected Reprint Series, New York.

Luhmann, N.C., and Peebles, W.A. (1984), *Rev. Sci. Instr.* **55**, 279.

Machuzak, J.S. (1986), Woskoboinikow, P., Mulligan, W.J., Cohn, D.R., Gerver, M., Guss, W., Mauel, M., Post, R.S., and Temkin, R.J., *Rev. Sci. Instr.* **57**, 1983.

Masi, C.G., and Phillips, T.G. (1986), *Test and Measurement World*, Vol. 60.

Mejia, S.R. (1985), McLeod, R.D., Pries, W., Shuftlebotham, P., Thomson, D.J., White, J., Shellenberg, J., Kao, K.C., and Card, H.C., *J. Non-Cryst. Solids* **77** and **78**, 765.

Meuth, H. (1986), in "Proceedings of SPIE- The International Society for Optical Engineering", Vol. 701, "Optics, Optical Systems and Applications", (A. Sona ed.).

Milligan, T.A. (1985), "Modern Antenna Design", McGraw-Hill, New York.

Milligan, T.A., and McDonnell, J. (1986), *Microwaves and RF* **25**, 103.

Minami, Kazuo, and Takeda, Susumu (1969), *Phys. Fluids* **12**, 1089.

Morgan, D.V., and Howes, M.J. (1980), in "Microwave Solid State Devices and Applications", Peter Peregrinus, New York.

Okabayashi, M., and Arunasalam, V. (1977), *Nucl. Fusion* **17**, 497.

Overzet,L.J., and Verdeyen, J.T. (1986), *Appl. Phys. Lett.* **48**, 695.

Paraszczak, J. (1985), Heidenreich, J., Hatzakis, M., and Moisan, M., *Microelectronic Eng.* **3**, 397.

Paris, P.J., and Hollenstein, Ch. (1983), *Rev. Sci. Instr.* **54**, 825.

Parker, J.V. (1964), Nickel, J.C., and Gould, R.W., *Phys. Fluids* **7**, 1489.

Podgornyi, I.M. (1971), in "Topics in Plasma Diagnostics", Plenum, New York.

Pollard, R.D. (1980), in "Microwave Solid State Devices and Applications", (D.V. Morgan and M.J. Howes, eds.), Peregrinus, New York.

Primich, R.I. (1965), Auston, D.H., Hayami, R.A., McLeod, J.D., and Zivanovic, S., in "Proceedings VIIth International Conference on Phenomena in Ionized Gases", Beograd, Vol. 3, p. 126.

Robson, P.N. (1969), Overmoded Rectangular Waveguides, in "Millimeter and Submillimeter Waves", (F.P. Benson ed.), Iliffe Books Ltd., London.

Roddy, D. (1986), "Microwave Technology", Prentice Hall, Englewood Cliffs.

Rohatgi, R. (1985), Chen, K.I., Bekefi, G., Kaplan, R.D., Luckhardt, S.C., Mayberry, M., Porkolab, M., and Villasenor, J.N.S., in "Proceedings of the 6th Topical Conference on RF Heating of Plasmas", Georgia.

Rutgers, W.R., and Boyd, D.A. (1977), *Phys. Lett.* **62A**, 498.

Sauthoff, N.R., and von Goeler, S. (1979), *I.E.E.E. Trans. Plasma Sci.* **PS-7**, 141.

Schulz, G.J., and Brown, S.C. (1955), *Phys. Rev.* **98**, 1642.

Severin, H. (1956), *I.R.E. Trans.* **AP4**, 385.

Sevillano, E. (1984), Brau, K., Goodrich, P., Irby, J., Mauel, M., Post, R.S., Smith, D.K., and Sullivan, J., *Rev. Sci. Instr.* **56**, 960.

Sheffield, John (1975), in "Plasma Scattering of Electromagnetic Radiation", Academic

Press, New York.

Shmoys, J. (1961), *J. Appl. Phys.* **32**, 689.

Slater, J.C. (1946), *Rev. Mod. Phys.* **18**, 441.

Somlo, P.I., and Hunter, J.D. (1985), "Microwave Impedance Measurements", Peregrinus, London, I.E.E.E. Electrical Measurement Series.

Stewart, R.D., and Robson, P.N. (1965), in "Proceedings VIIth International Conference on Phenomena in Ionized Gases", Beograd, Vol. 3, p. 109.

Strawitch, C. (1986), Yujiri, L., Richardson R., and Lang, A., *Bull. Am. Phys. Soc.* **31**, 1543.

Suvorov, E.V. (1984), Fedyanin, O.I., Fraiman, A.A., and Kholńov, Yu.V., *Sov. J. Plasma Phys.* **10**, 73.

Tallents, G.J. (1984), *J. Phys. D:* **17**, 721.

Taylor, G. (1985), Efthimion, P.C., McCarthy, M., Fredd, E., Goldman, M.A., and Kaufman, D., *Rev. Sci. Instr.* **56**, 928.

Taylor, G. (1986), Efthimion, P.C., McCarthy, M.P., Fredd, E., and Cutler, R.C., *Rev. Sci. Instr.* **57**, 1974.

Tonks, L. (1931), *Phys. Rev.* **37**, 1458; *Phys. Rev.* **38**, 1219.

Tsukishima, Takashige (1979), in "Diagnostics for Fusion Experiments", (E. Sindoni and C. Wharton, eds.), Pergamon Press.

Uckan, T. (1981), *Rev. Sci. Instr.* **52**, 21.

Uckan, T. (1983), *Rev. Sci. Instr.* **54**, 1420.

Uckan, T. (1984), *Rev. Sci. Instr.* **55**, 1874.

Vadnjal, M., and Buffa, A. (1965), in "Proceedings VIIth International Conference on Phenomena in Ionized Gases", Beograd, Vol. 3, p. 105.

Vainstein, L.V. (1963), *Zhurn. Exp. Teor. Fiz.* **44**, 1050.

Walker, B. (1981), Baker, E.A.M., and Costley, A.E., *J. Phys. E:* **14**, 832.

Wallington, J.R., and Beynon, J.D.E. (1969), *J. Plasma Phys.* **3**, 371.

Wetzer, J.M. (1983), *I.E.E.E. Trans. Plasma Sci.* **PS-11**, 72.

Wharton, C.B. (1957), UCRL Report 4836.

Wharton, C.B. (1965), "Microwave Techniques" in "Plasma Diagnostic Techniques", (R.H. Huddlestone and Stanley L. Leonard, eds.), Academic Press, New York.

	$\mathcal{E}_1$	$\mathcal{F}_1$	$\mathcal{F}_2$	$\mathcal{H}_2$	$\mathcal{G}_1$	$\mathcal{G}_2$	
E_z	J_m	$-J_m$	$-Y_m$	eJ_m			r_o
H_φ	$k\mathcal{A}_2 h + \omega\epsilon_o \mathcal{B}_2$	$-\omega\epsilon_o \mathcal{K}_1^1$	$-\omega\epsilon_o \mathcal{K}_1^2$	$k\mathcal{A}_2 + \omega\epsilon_o \mathcal{B}_2 e$	$-k\mathcal{K}_2^1$	$-k\mathcal{K}_2^2$	r_o
E_z		J_m	Y_m				r_c
H_z	hJ_m			J_m	$-J_m$	$-Y_m$	r_o
E_φ	$k\mathcal{A}_2 - \omega\mu_o \mathcal{A}_1 h$	$-k\mathcal{K}_2^1$	$-k\mathcal{K}_2^2$	$k\mathcal{A}_2 e - \omega\mu_o \mathcal{A}_1$	$\omega\mu_o \mathcal{K}_1^1$	$\omega\mu_o \mathcal{K}_1^2$	r_o
$\partial_r H_z$					J_m'	Y_m'	r_c
	κ_1	κ_v	κ_v	κ_2	κ_v	κ_v	

Table I

FIGURE CAPTIONS

Figure 1. Microwave measurements that characterize a device under test (DUT).

Figure 2. The three independent components of the dielectric tensor for a cold plasma vs. frequency.

Figure 3. Wave coupling in the boundary: surface waves (a) plasma motion stops at the boundary. (b) Plasma swings through the boundary.

Figure 4. Geometry for microwave interferometry.

Figure 5. Radial plasma profiles in a cavity or waveguide: (a) parabolic, (b) power-law (right half), and equivalent rectangular (left half) profile.

Figure 6. Common cavity configurations.

Figure 7. Swept-frequency interferometer schematic.

Figure 8. Quadrature phase detector schematic.

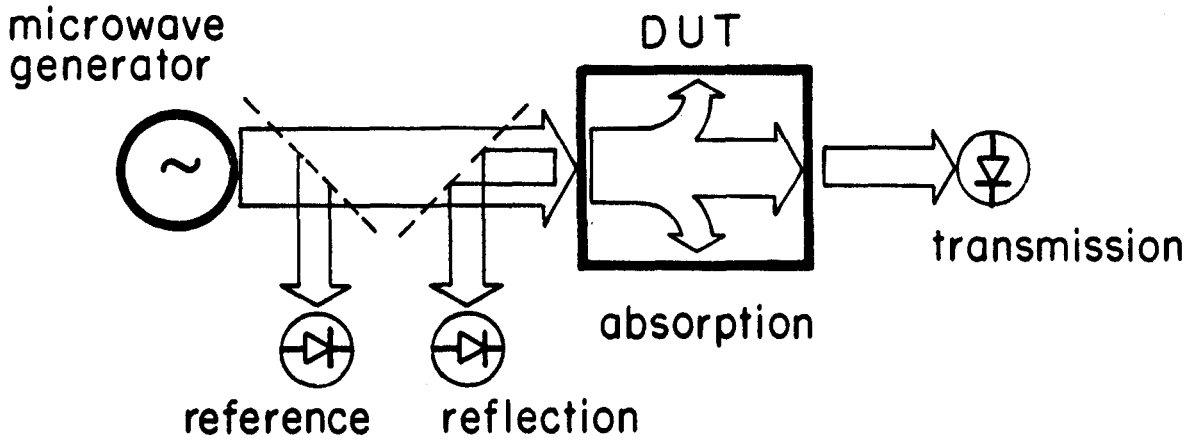
microwave
generator
DUT
transmission
absorption
reference
reflection

Figure 1

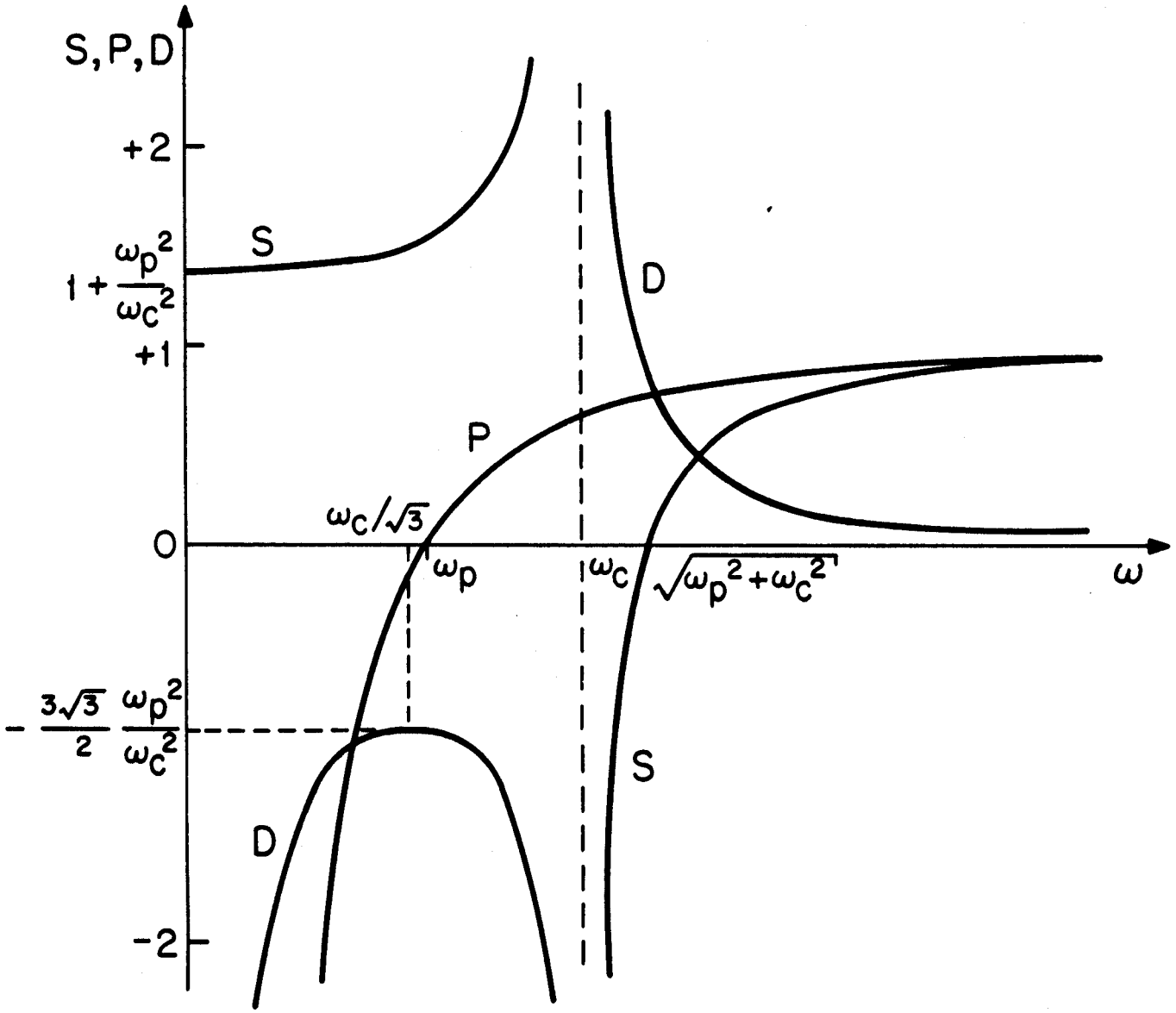
S, P, D
+2
$1+\frac{\omega_p^2}{\omega_c^2}$
+1
0
$-\frac{3\sqrt{3}}{2}\frac{\omega_p^2}{\omega_c^2}$
-2
S
D
P
D
S
$\omega_c/\sqrt{3}$
ω_p
ω_c
$\sqrt{\omega_p^2+\omega_c^2}$
ω

Figure 2

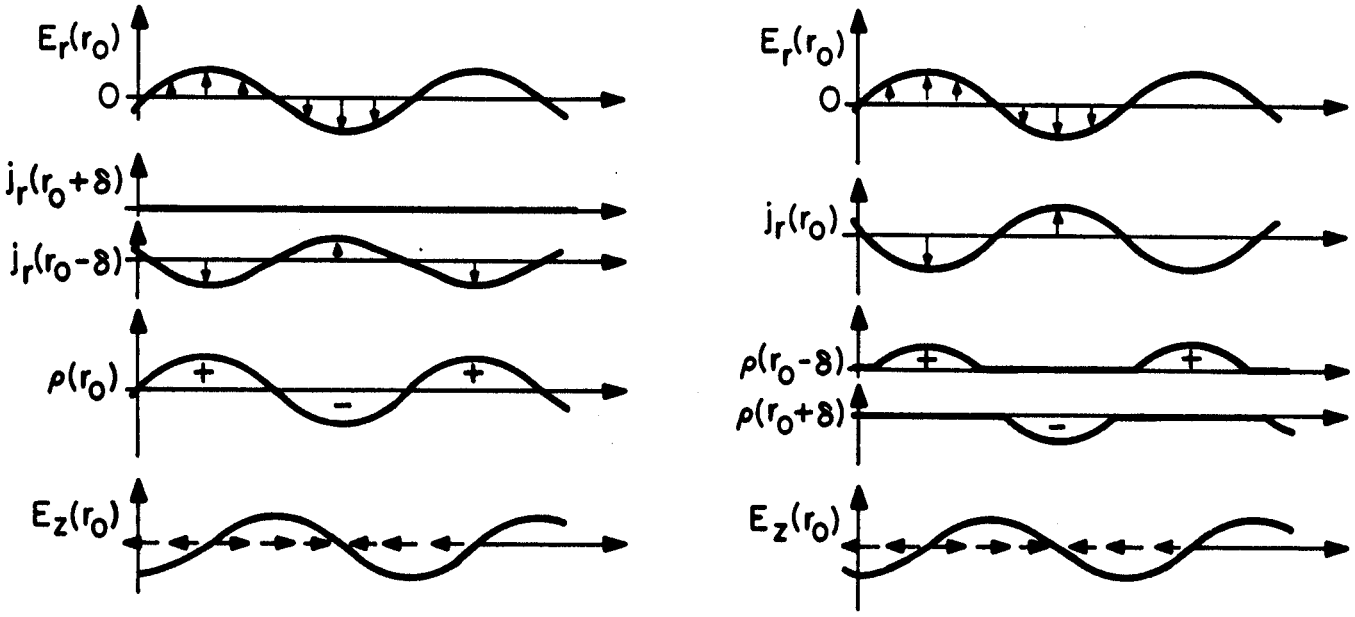
$E_r(r_o)$
0
$j_r(r_o+\delta)$
$j_r(r_o-\delta)$
$\rho(r_o)$
+
−
+
$E_z(r_o)$
$E_r(r_o)$
0
$j_r(r_o)$
$\rho(r_o-\delta)$
+
+
$\rho(r_o+\delta)$
−
$E_z(r_o)$

Figure 3

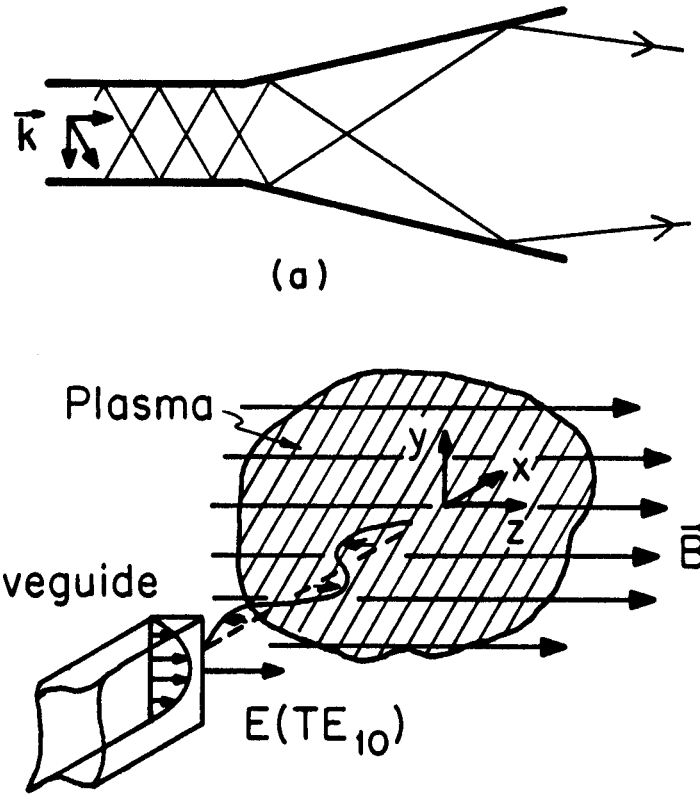

Figure 4

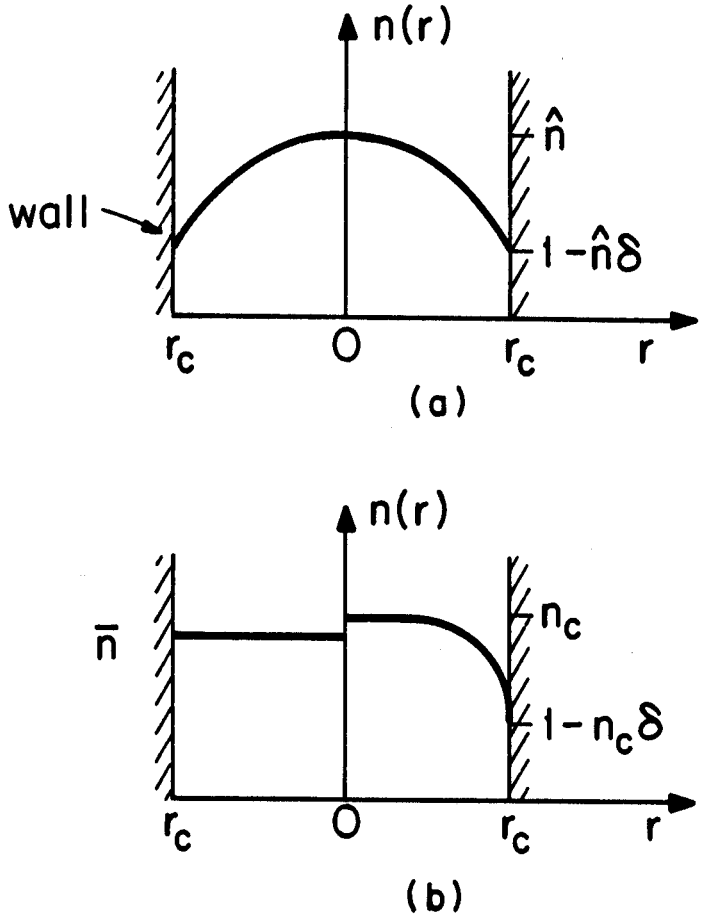
n(r)
wall
$\hat{n}$
$1-\hat{n}\delta$
r_c
O
r_c
r
(a)
n(r)
$\bar{n}$
n_c
$1-n_c\delta$
r_c
O
r_c
r
(b)

Figure 5

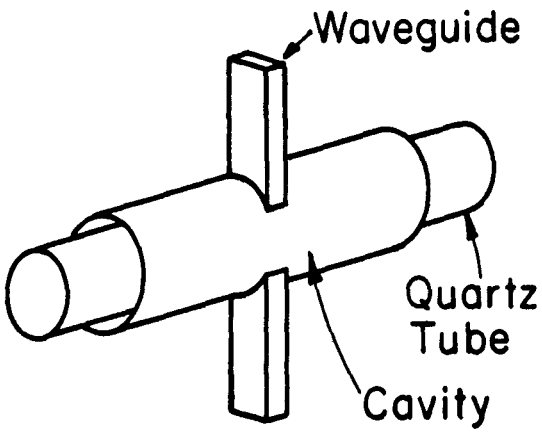

(a)

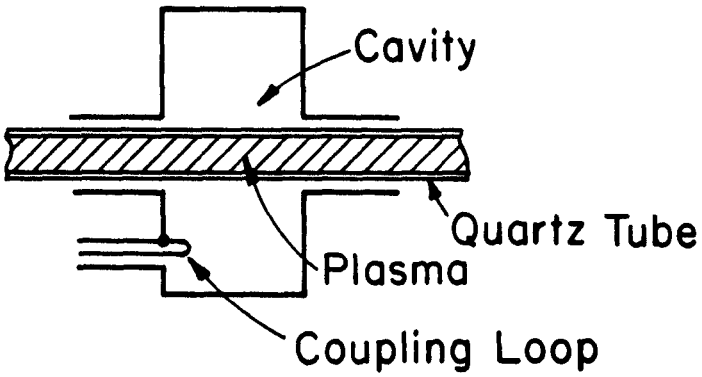

(b)

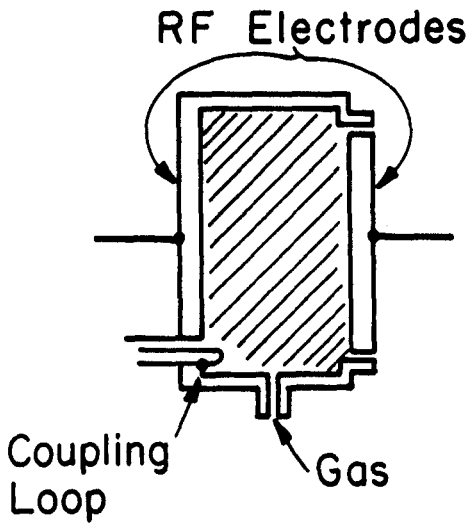

(c)

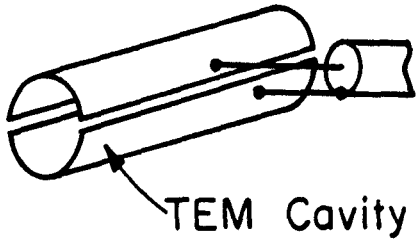

(d)

Figure 6

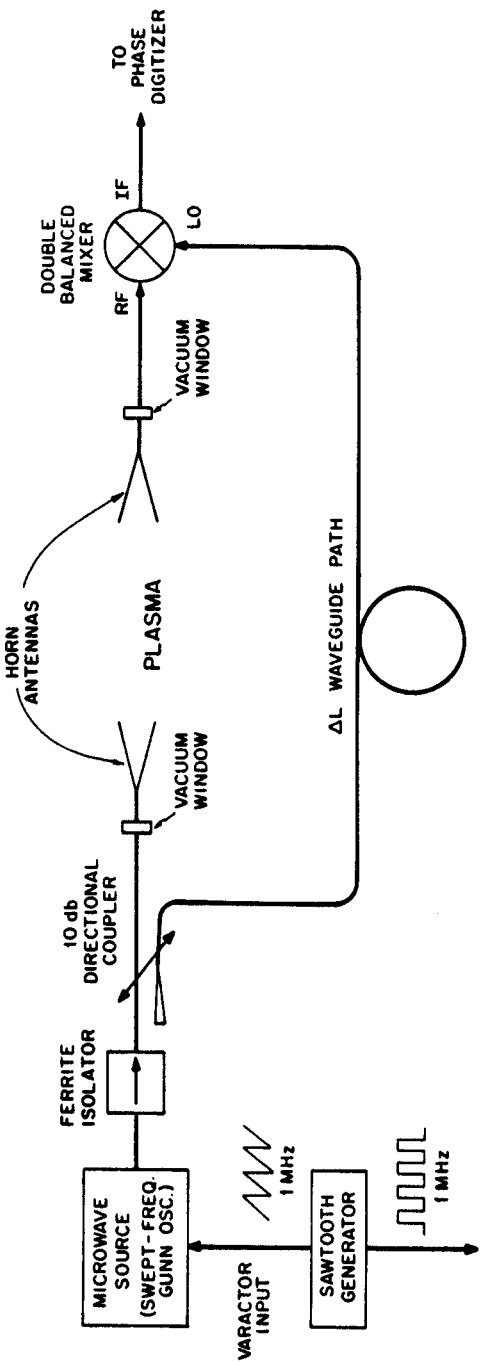
TO PHASE DIGITIZER
IF
LO
DOUBLE BALANCED MIXER
RF
VACUUM WINDOW
HORN ANTENNAS
PLASMA
ΔL WAVEGUIDE PATH
VACUUM WINDOW
10 db DIRECTIONAL COUPLER
FERRITE ISOLATOR
MICROWAVE SOURCE (SWEPT-FREQ. GUNN OSC.)
1 MHz
VARACTOR INPUT
SAWTOOTH GENERATOR
1 MHz
TO PHASE DIGITIZER

Figure 7

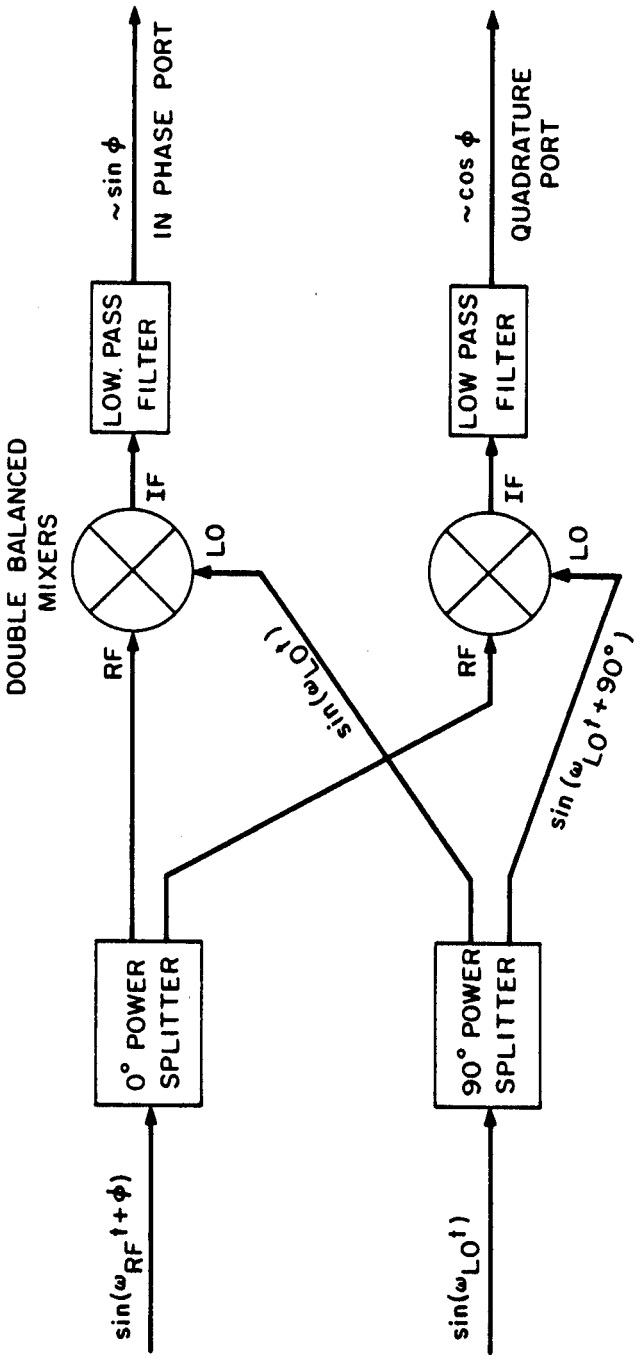
DOUBLE BALANCED MIXERS
RF
LO
IF
LOW PASS FILTER
~sin φ
IN PHASE PORT
~cos φ
QUADRATURE PORT
0° POWER SPLITTER
90° POWER SPLITTER
sin(ω_RF t + φ)
sin(ω_LO t)
sin(ω_LO t)
sin(ω_LO t + 90°)

Figure 8